1994

8 Deep sea processes of sediment transport and deposition

D.A.V. STOW

8.1 Introduction

8.1.1 Definitions

For the purposes of this chapter, we can define all sedimentary environments that occur below storm wave base (approximately 200 m water depth) as deep sea. This provides us, therefore, with a very large playground in which to operate, including all areas of oceans and marginal seas beyond the shelf-slope break, and hence beyond the reach of most processes discussed in other chapters in this book. The shelf edge typically occurs at depths of about 100–200 m, although locally it may be as shallow as 20 m and so well within the influence of waves and tidal currents. Enclosed and semi-enclosed basins, on broad shelf areas or in the central parts of fjords, may also provide sites of sedimentation below wave base.

Collectively, these areas present a remarkable variability in: (1) *physiography* — including narrow deep-sea trenches, broad flat abyssal plains, gentle gradients of open slopes, steep margins off reef complexes and volcanic seamounts, and irregular topography associated with mid-ocean ridge zones; and (2) *tectonic setting* — including active convergent and oblique slip margins such as those surrounding much of the Pacific Ocean, mature divergent margins that typify both the west and east Atlantic, arc-related and more complex marginal basins such as the Mediterranean Sea, and young rift basins such as the Red Sea. Consequently, there is an equal range of bathymetry and scale, as well as variety of processes that operate and factors that control them.

For clastic sedimentary particles to accumulate in the deep sea they must be eroded from land or from the sea floor, be transported beyond the shelf-slope break, and then deposited. Much biogenic material is synthesized directly in the oceans and then subjected to similar transport–depositional processes, although biogenic detritus may also be derived by erosion. Authigenic minerals are precipitated directly from sea water at or near the sediment–water interface, and they too may be subsequently reworked.

In this chapter, we first of all consider the origin and supply of sedimentary materials to the deep-sea realm, the fluids and forces that act within this milieu, and then define the range of processes that operate to redistribute the materials supplied. We then discuss each of the main processes in turn, the typical bedforms they generate and characteristic properties of the sediments deposited. A final section outlines the main allocyclic and autocyclic controls that influence these processes.

The data presented draw heavily on previous syntheses of deep-water processes (e.g. Stow, 1985, 1986, 1992; Pickering *et al.*, 1989) as well as the most recent literature on the subject.

8.1.2 Sediment supply

The primary source of terrigenous material in deep-sea deposits is the physical and chemical weathering and erosion of pre-existing rocks. The nature and rate of supply will be affected principally by tectonic, climatic and sea-level controls in the source and transitional regions. Collectively, the world's rivers transport by far the largest volume of suspended and dissolved loads to the sea, most of the former being deposited initially in paralic and shallow shelf environments. At high latitudes, melting and calving from glaciers and floating ice adds directly to both shelf and deep-sea deposition. Eolian processes can

Table 8.1 Sediment flux to the ocean basins

Source	*Supply* $\times 10^9$ *t year*$^{-1}$
Rivers (suspended load)	18.3
Rivers (solution load)	4.2
Groundwater (solution load)	0.48
Ice (ice shelves and bergs)	3.0
Coastal erosion	0.25
Wind-blown dust	0.6
Volcanic ejecta	0.15
Biogenic carbonate	1.4
Biogenic silica	0.49

Data from Goldberg (1974) and Open University (1984).

Table 8.2 Principal properties of sea-water

Salinity:	
General average	35‰
Surface waters	32.4–39.8‰
Deep water (>1000 m)	34.5–35‰
Temperature	
General average	3.52°C
Surface range	- 1.87°–30.0°C
Deep water (>1000 m)	- 3.56°–8.9°C
Density	
(expressed as specific gravity)	1.024–1.029
pH	
General average	8.0

contribute large volumes of finer grained material derived from low latitude arid and semi-arid regions as well as from explosive volcanic eruptions.

The relative flux from these different sources is poorly constrained at present (Table 8.1) and will have varied markedly in the past.

Biogenic material, including calcareous and siliceous tests as well as soft organic tissue, is supplied from primary productivity in surface waters of the oceans and seas, from organic growth in shoal areas followed by erosion and resedimentation, and as runoff from biogenic-rich areas of the continents and coastline (e.g. swamps and rainforests, river biota, shoreface molluscs, etc.). Calculating the flux of this material is even more complex than for terrigenous flux, as so much is dissolved and recycled, often many times over, before reaching the deep-sea floor.

The oceans are truly a chemical soup with an ionic composition built up from the dissolved loads of fluid input, dissolution of biogenic material following death of the organism, progressive corrosion of unstable clastic components such as ferromagnesian minerals, feldspars and amorphous compounds, and primary volcanic/hydrothermal emissions from mid-ocean ridges. There appears to be a crude steady state chemistry within the oceans, involving large material flux in and out of solution.

8.1.3 Fluids and forces

Sea-water properties

The ambient fluid in the oceans is sea water, having physical and chemical characteristics that lie within certain well-defined limits (Table 8.2).

Although it is not possible to isolate the deep sea as a separate fluid, when the average mixing time of the oceans is in the order of 1500 years, the oceans can be considered in terms of distinct water masses that have recognizable and measurable parameters and that show progressive mixing across their boundaries.

Physical forces

The physical forces that have most affect on deep-sea water, both within and between the separate water masses, include: (1) temperature and salinity differences that drive the thermohaline circulation; (2) internal tides and waves; (3) the Coriolis force that acts on moving water masses; (4) sea surface topography coupled with major storm events that transmit surface potential energy downwards through the water column; and (5) sediment suspensions held in semi-permanent nepheloid layers and in episodic sediment gravity flows that move by virtue of the downward acting gravitational force.

The sea-water/sediment interface acts as a critical transition zone in the deep sea, and is very variable from one area to another. In some mud-rich areas it has a soft spongy texture with 70–80% water content and full interchange with the superjacent fluid; in others, it has been swept and winnowed repeatedly by strong bottom currents leaving a coarse sand or gravel lag substrate. Incipient cementation may produce hard grounds on carbonate bottoms, whereas precipitation of ferromanganese compounds may result in nodules and pavements.

The sediments below the sea floor act as an enormous reservoir for porewaters (approximately equal to 20% of the ocean volume), and show continuous interchange with the ocean reservoir across the water/sediment boundary.

The initiation of movement in various particulate materials on the sea floor, both from the margins into the deep sea and within the ocean basins, can be considered in terms of (1) the mechanics of sediment failure on a slope; or (2) the critical shear velocity required to erode and move sedimentary materials on a plane bed.

In the first case, sediment deposited on a slope will only begin to move downslope when the shear stress exerted by the force of gravity exceeds the shear strength of the sediment (Watkins & Kraft, 1978; Karlsrud & Edgers, 1982) along a slip plane within the sediment column (Fig. 8.1(a)). The shear strength is a function of the cohesion between the grains plus the intergranular friction. Sediment failure therefore results either from an increase in shear stress, due to a steepening of the slope or thickening of the sediment pile, or from a decrease in shear strength due to the sudden shock of earthquakes, storms, etc., causing fluidization or thixotrophy in the sediment. The weight of rapidly deposited sediments may exert a similar strain effect.

In the second case, sediment lying on a plane bed will begin to move as the fluid shear stress is increased and the critical threshold for grain movement is reached. Each sediment grain will experience a drag force due to the fluid shear velocity at the bed and a lift force due to the Bernoulli effect. When these combined fluid forces exceed the normal weight force due to gravity the grain will begin to move (Fig. 8.1(b)). Storms, internal waves, normal bottom currents and turbidity currents can all initiate sediment movement in this way.

Various experimental investigators have attempted to determine the threshold of motion for different grain types and sizes. The much used Hjulstrom (1939) diagram relating erosion of a particular grain size to current velocity (Fig. 8.1(c)) is poorly established and incorrect for grain sizes finer than

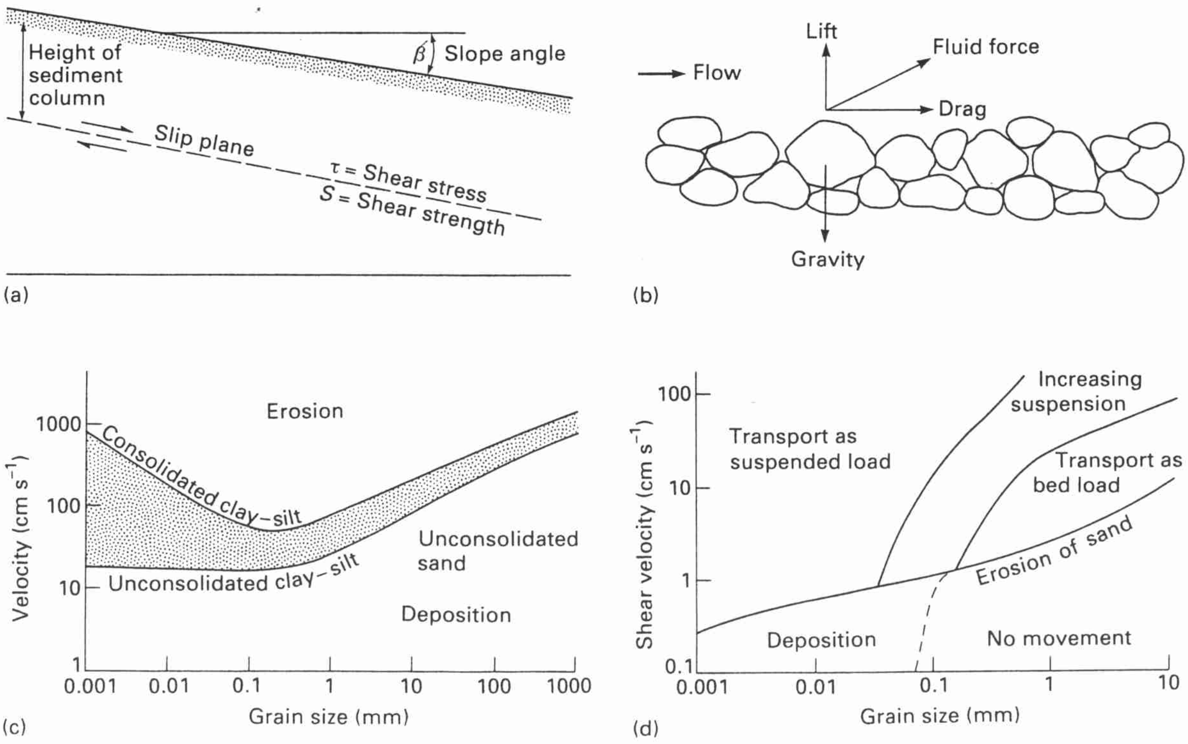

Fig. 8.1 Erosion, transport and deposition of sedimentary materials. (Stow, 1986).

sands. Shields (1936) related the grain Reynolds number to a dimensionless shear stress, but also had few data for the finer grain sizes, whereas Miller *et al.* (1977) present much better data in this size range. A more recent synthesis (McCave, 1984) plots grain size against shear velocity showing transport–deposition fields for fine sediment and transport–erosion fields for coarser materials (Fig. 8.1(d)). McCave argues that erosion of fine cohesive sediment is not simply a function of grain size and velocity and cannot therefore be plotted on the same diagram.

Once in the water column and on the move, then a range of different forces and processes acts to further transport and eventually deposit sedimentary material. These processes are discussed in detail in the following sections.

Chemical forces

Various chemical forces must also be taken into account as they can very significantly affect certain types of deep-sea sediment. Below the carbonate compensation depth (CCD), bottom waters are highly aggressive (i.e. having low pH values) towards both biogenic and inorganic carbonate material such that, unless deposition and burial is extremely rapid, all $CaCO_3$ will be dissolved either in the water column and/or on the sea floor. Only an insoluble silicate residue will be preserved as sediment.

The depth of the CCD in modern oceans is a function of biogenic productivity, oceanic circulation and the geochemical cycle of carbon. It averages 5.3 km in the North Atlantic, decreasing to 4.4 km in the North Pacific, and has varied markedly in the past. The aragonite compensation depth (ACD) is generally about 1 km shallower.

Biogenic opaline silica is chemically unstable throughout the water column but both rapid sedimentation and protection by a thin organic film surrounding the siliceous tests allows its accumulation in certain parts of the deep sea. Most organic matter is rapidly oxidized and recycled during its descent through the water column but preservation in the sediment can result from very high rates of production and/or the development of zones with anoxic (or very low oxic) bottom waters. This generally acts to suppress biological degradation of organic material.

Different chemical environments in the deep sea can also lead to authigenic precipitation of certain minerals including clays, zeolites, ferromanganese crusts, phosphates and carbonate hardgrounds.

Biological forces

Biological forces that influence deep-water sediments either prior to and/or post-deposition include: (1) primary productivity, which has a direct affect on sediment supply and on chemical partitioning in the oceans; (2) bacterial decay processes, which serve to alter the organic component of sediment once deposited and hence also affect the pore water chemistry; and (3) the activity of burrowers and borers on and within sediments, which mix and homogenize, stir and suspend or break down and erode almost any substrate that is left uncovered for even relatively short periods of time.

The range of processes

Within the deep sea, three main groups of processes are capable of eroding, transporting and depositing terrigenous, biogenic, volcanigenic and other particulate materials (Fig. 8.2): *resedimentation processes*, *bottom currents* and *surface currents with pelagic settling*. For completeness we have added *authigenic processes* on Fig. 8.2, recognizing the *in situ* origin of some deep-sea materials. Several attempts have been made to classify these processes, so that a plethora of terminology and confusing (partial) synonyms exists (see review by Nardin *et al.*, 1979). The classification in Table 8.3 is based on the mechanical behaviour of the flow, the transport mechanisms and sediment support system (Dott, 1963; Middleton & Hampton, 1976; Moore, 1977; Lowe, 1979; Nardin *et al.*, 1979; Pickering *et al.*, 1989).

The 15 conceptually distinct processes listed (not including authigenic processes), are in fact part of a continuum of mechanical behaviour, ranging from elastic through plastic to viscous fluid and viscous settling (Fig. 8.3). The transition from slides to sediment gravity flows involves a change in the physical state of the sediment mass towards greater internal disaggregation by breakdown of the metastable grain packing and incorporation of more fluid. The transition from debris flow to liquefied or fluidized flows and turbidity currents involves further remoulding and dilution of the flow. During any single event of transport and deposition (Fig. 8.3) these various processes may operate at the same time or in temporal sequence, as demonstrated experimentally (Middleton, 1967) and from field evidence (Hein, 1982).

The extreme end member of sediment gravity flows, a very low-concentration, low-velocity turbidity current will be deflected by the Coriolis force from its downslope path to a direction along the slope. At this point it may grade imperceptibly into a normal bottom current, also known as a contour current, which is driven by the deep thermohaline circulation in the oceans (Stow & Lovell, 1979) rather than by the gravitational effect of its sediment load. Other bottom currents (Fig. 8.2) are also caused by normal oceanic circulation, and all behave as viscous fluids. When there is no horizontal advection and dilution is extreme, simple vertical settling of particles occurs. The influence of sediment-free or non-depositing bottom currents may be important in supplying dissolved chemical species for authigenic mineral growth in some instances.

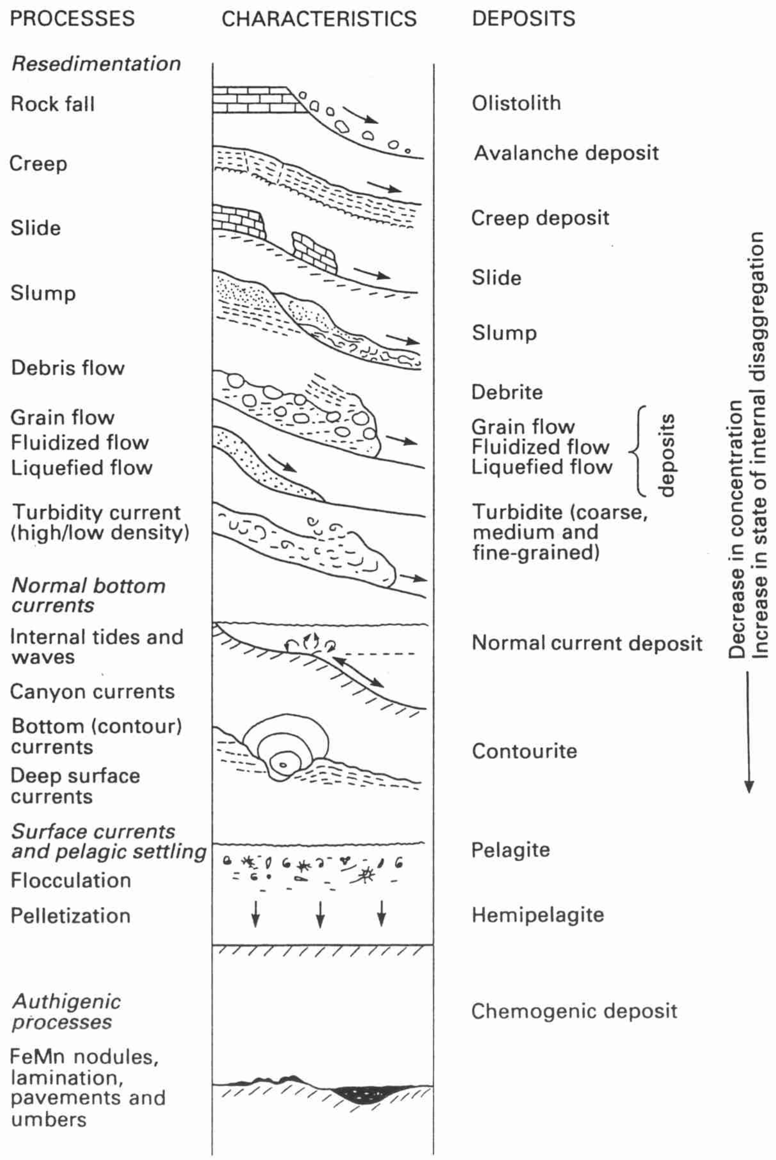

Fig. 8.2 The range of processes that operate in the deep sea. (Stow, 1986.)

Table 8.3 Definitions of depositional processes in the deep sea (modified from Nardin *et al.*, 1979) and estimates of their chief physical characteristics. Reprinted from Stow (1986)

Depositional process	*Transport and sediment support mechanisms*	*Slope*	*Dimensions*	*Concentration*	*Velocity* ($cm\ s^{-1}$)	*Duration*	*Transport distance (km)*	*Average sedimentation rate*
RESEDIMENTATION†	*Elastic**							
Rock fall	Freefall and rolling of blocks and clasts, no internal deformation of clasts	Very steep	Clasts can be >10 m	Solid	Freefall	?min to h	<0.5	High
Sediment creep	Slow strain and downslope movement along decollement zone due to load-induced stress with little internal deformation	Gentle	20–80 m thick	'Solid'	V. slow (imperceptible)	Semi-continuous	?<0.5	As for background
Slide (glide)	Shear failure along discrete shear planes with little internal deformation	>About 1°	Max. 300 km^3, 500 m thick (+complete range)	Almost 'solid'	?	?h	0.001–?100	High
Slump	Shear failure accompanied by rotation along discrete shear surfaces	>About 1°	As above	Almost 'solid'	?	?h	0.001–?100	High
	*Plastic**							
Debris flow (mudflow)	Shear distributed throughout sediment mass, slow plastic flow, clast buoyancy and matrix strength support mechanisms	>About 1°	Up to few 10s of m thick	Dense slurry	?1–20	?h	?Max 350	Moderate to high
	*Viscous fluid (flow)**							
Grain flow	Quasi-visco-plastic flows of cohesionless grains, dispersive pressure support mechanism, localized, small-scale events	>18°	Up to few cm thick	Few data available	Few data available	?min to h	?<0.1	Do not usually operate as separate processes
Fluidized flow	High-viscosity, short-lived flow of cohesionless grains, supported by upward-moving pore waters	>3°	<10 cm thick	Few data available	Few data available	?min to h	?<0.1	Do not usually operate as separate processes
Liquefied flow	Cohesionless sediment supported by upward-escape of pore waters as flow collapses and freezes, very short-lived	>About 0.5°	Basal few 10 cm of flow	Few data available	Few data available	?min to h	?<0.05	Do not usually operate as separate processes

Turbidity current (high density)	Low-viscosity flow of mixed grains supported by fluid-turbulence (autosuspension)	>About 0.5°	Length and width up to 10s of km, thickness up to 100 s of m	50–250 g l^{-1}	Max. 250	?h to about 1 day	Up to about 1000	<5 cm to >5 m per 1000 years
Turbidity current (low density)	Very low-viscosity flow of mixed grains supported by fluid turbulence (autosuspension)	Almost no slope	As above	0.025–3 g l^{-1}	Average 10–50	?h to few days	Up to several 1000s	<5 cm to >5m per 1000 years
NORMAL BOTTOM CURRENTS‡								
Internal tides and waves	Medium to large-scale oscillations at density discontinuities within upper few hundred metres of water column, can suspend sediment by fluid turbulence	No slope	Up to few 10s of m amplitude	?	5–300	Semi-continuous currents often with marked periodicities	?	V. low
Normal canyon currents	Essentially 'clear-water' flows, up and down slope canyons and channels, tidal or higher periodicity, minor sediment suspension by fluid turbulence	Up and down slope <few°	Up to few 10 s of m thick	?<0.3 mg l^{-1}	0–30	Semi-continuous currents often with marked periodicities	Up to several 100s	Low
Bottom (contour) currents	Deep, slow, essentially 'clear-water' flows driven by thermohaline circulation, can be associated with bottom nepheloid suspensions (fluid turbulence)	No slope or gentle slopes	Width up to few 10s of km, thickness up to 100s of m	0.025–0.25 mg l^{-1}	Max. 200 Mean 10	Semi-continuous currents often with marked periodicities	Up to several 1000s	<10cm per 1000 years
Deep surface currents	Deep, slow, essentially 'clear-water' flows that are deep parts of surface wind-driven ocean currents	No slope or gentle slope	As above	?As above		Semi-continuous currents often with marked periodicities	?As above	
PELAGIC SETTLING	*Viscous fluid**							
Pelagic settling	Vertical settling of individual grains, flocs and pellets through water column (viscous fluid)	Ubiquitous	Settling through 100s to 1000s of m water column	Extremely low	0.002–0.005 settling rate (or more if flocs)	Semi-continuous	No horizontal transport	Mean <1 cm per 1000 years

* Mechanical behaviour; † resedimentation (= mass gravity transport); ‡ normal bottom currents (= semi-permanent bottom currents).

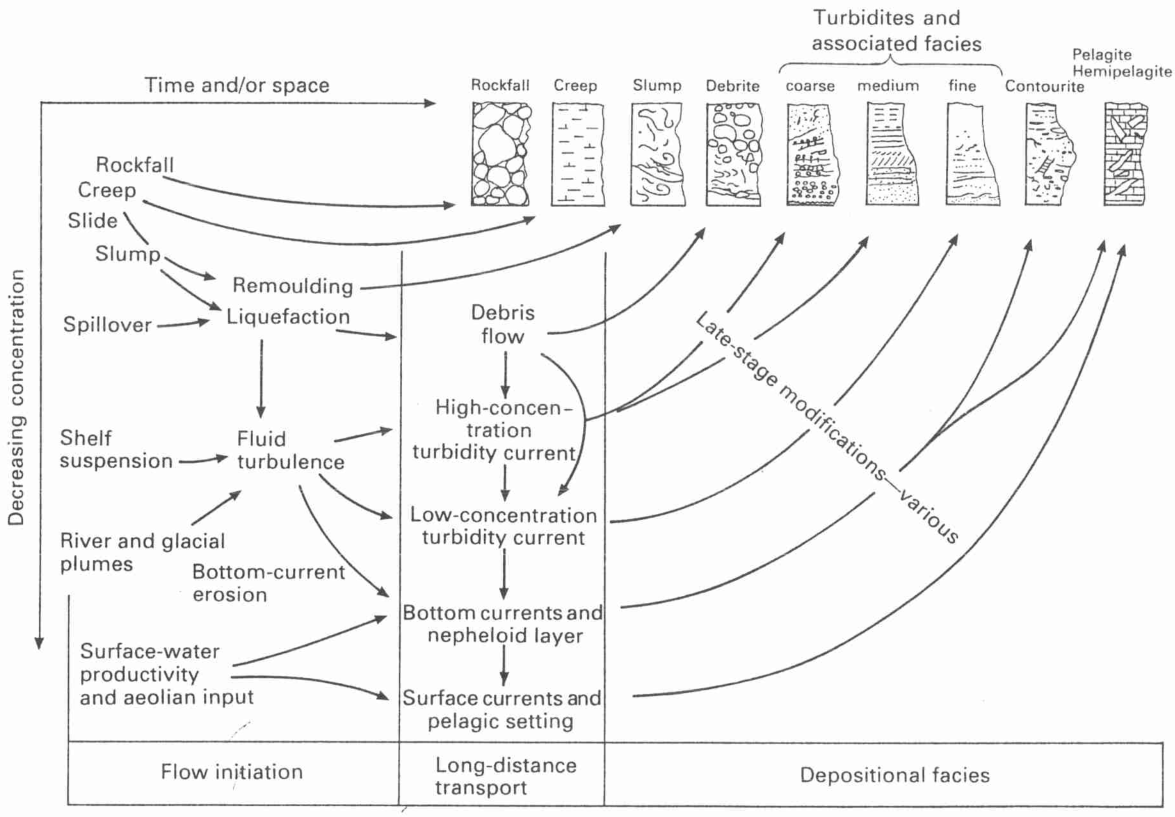

Fig. 8.3 Deep-sea process interaction and continuum in relation to main sedimentary deposits. Framework is one of time and/or space, and concentration of flows. Idealized facies models that result from deposition by the different processes are also shown. Post-depositional modification can involve current reworking, liquefaction and bioturbation. (From Pickering, Stow *et al.*, 1986; modified after Walker, 1978.)

8.2 Resedimentation processes

8.2.1 Introduction

Resedimentation processes (including both *mass gravity transport* and *sediment gravity flow*) are all those processes that move sediment downslope over the sea floor from shallower to deeper water and are driven by gravitational forces (Fig. 8.2, Table 8.3). Many of these processes have close analogues with downslope processes on land and with pyroclastic processes associated with explosive volcanic eruptions, both of which have been the subject of intensive study by geomorphologists, engineers and volcanologists, as well as by sedimentologists. Our understanding of the deep-sea equivalents is being slowly pieced together through laboratory experiments, a growing body of direct observational data and by careful scrutiny of the resultant deposits.

It is clear that many of the resedimentation processes are extremely complex in nature and do not lend themselves readily to mathematical modelling, although we have tried to present the current state-of-the-art in the following pages. Three important properties we should mention at the outset are mechanical behaviour, cohesiveness of the debris involved and sediment-support mechanisms.

Mass movements such as rockfall, creep and slides, are characterized by generally elastic behaviour in which strain is directly proportional to stress and material displacement occurs without significant internal deformation. Debris flows behave plastically, with shear deformation being distributed throughout the moving wet sediment mass. Sediment gravity flows, including grain flow, fluidized flow, liquefied flow and turbidity currents, exhibit viscous fluid behaviour, ranging from very high viscosity (quasi-viscous) to very low viscosity flows.

In nature, the material involved may be entirely granular or cohesionless (e.g. sand, gravel) or dominantly cohesive (e.g. mud, clay), and this will influence the style of behaviour and movement. Muddy sediment is more likely to creep or slide downslope than move as a rockfall. Sandy debris flows, exhibiting mainly frictional strength and grain collision support mechanisms, will flow less far than muddy (cohesive) debris flows. Of course, many natural flows display a mixed granular–cohesive behaviour.

Downslope movement or flow of sediment–water mixes will continue provided that the shear stress generated by movement exceeds frictional resistance to flow, and that the grains or clasts are inhibited from settling by one of several support mechanisms (Pickering *et al.*, 1989). These mechanisms include: (1) turbulence of the fluid, at high Reynold's numbers and Froude numbers greater than unity; (2) buoyancy provided by a high density flow matrix; (3) dispersive pressure generated from grain collisions; (4) trapped or escaping pore fluids creating an upward fluid drag; and (5) internal strength, either frictional or cohesive, of the moving sediment mass. Natural resedimentation events commonly display an interaction of support mechanisms (Table 8.3).

8.2.2 Rock falls and avalanches

Rock falls are sudden, rapid, freefall events that are common in mountainous areas on land or along sea cliffs but are relatively rare at sea because the slopes are mostly too gentle. They occur only on steep slopes of faulted or carbonate margins or in the heads of deeply incised submarine canyons, and are initiated by undercutting and erosion, and by earthquake shocks. Single displaced clasts (olistoliths) may be very large (> 10 m) and bounce or roll downslope for several tens or hundreds of metres before coming to rest (Johns, 1978). Talus slopes are common off reef mounds and poorly sorted, loose carbonate debris is well known from many ancient and modern carbonate margins where the slope angle is around 30° or more (Kenter, 1990). A combination of rock fall, rock avalanche, sliding and grain flow is believed responsible for such deposits.

Shor *et al.* (1990) have described gravel/boulder scree deposits from submersible dives along a steep, eroded, thalweg margin within the main Laurentian Fan channel. These were derived from loose gravel wave deposits on the main floor of the incised channel.

8.2.3 Sediment creep

Sediment creep is a process of slow strain due to load-induced stress (or the downslope weight of sediment), that may extend over periods ranging from hours to thousands of years (Watkins & Kraft, 1978). It is most commonly observed as *soil creep* down hillslopes on land, for which Carson and Kirkby (1972) recognize two classes of mechanism.

Continuous or rheological creep occurs as a result of the constant breaking and reforming of the tiny electrochemical bonds between individual particles. The cumulative effect of this is very slow downslope creep. *Intermittent* creep (usually diurnal or seasonal) is the result of physical or biological displacement of particles, at first normal to the slope and then with a downslope readjustment. Heating and cooling, wetting and drying, freezing and thawing are all mechanisms that cause soil creep, but seem unlikely to act on deep-water sediments. Burrowing organisms, coupled with internal slippage, suspension transport within the soil of the finest particles, and rheological creep most probably dominate on submarine slopes.

With so many mechanisms combining to determine the final sediment movement, it is difficult to derive a mathematical model for creep. However, Allen (1985) derived a model for soil creep in which the creep rate, U, at depth, y, is given by:

$$U = U_o - \frac{(\gamma_g \sin \beta)}{2\eta_a} y^2, \qquad (8.1)$$

where U_o is the surface creep rate, γ is the soil bulk density, β is the slope angle, η_a is the apparent viscosity of soil (held constant).

Allen (1985) found that the velocity profile given by Eq. 8.1 was not especially like observed profiles. He therefore introduced an exponential increase in the apparent viscosity with depth and derived a model giving more realistic results, noting that some movement was predicted at all depths.

Interestingly, Hill *et al.* (1982) interpreted seismic records of a compressionally folded, surface unit on the Canadian Beaufort Sea slope as indicating downslope creep of the upper few tens of metres with displacement at depth being taken up by movement along an internal decollement zone (Fig. 8.4).

Few other direct observations of submarine sediment creep have been made so that the processes, rates of movement, thickness of section involved, and the conditions that most favour creep are little

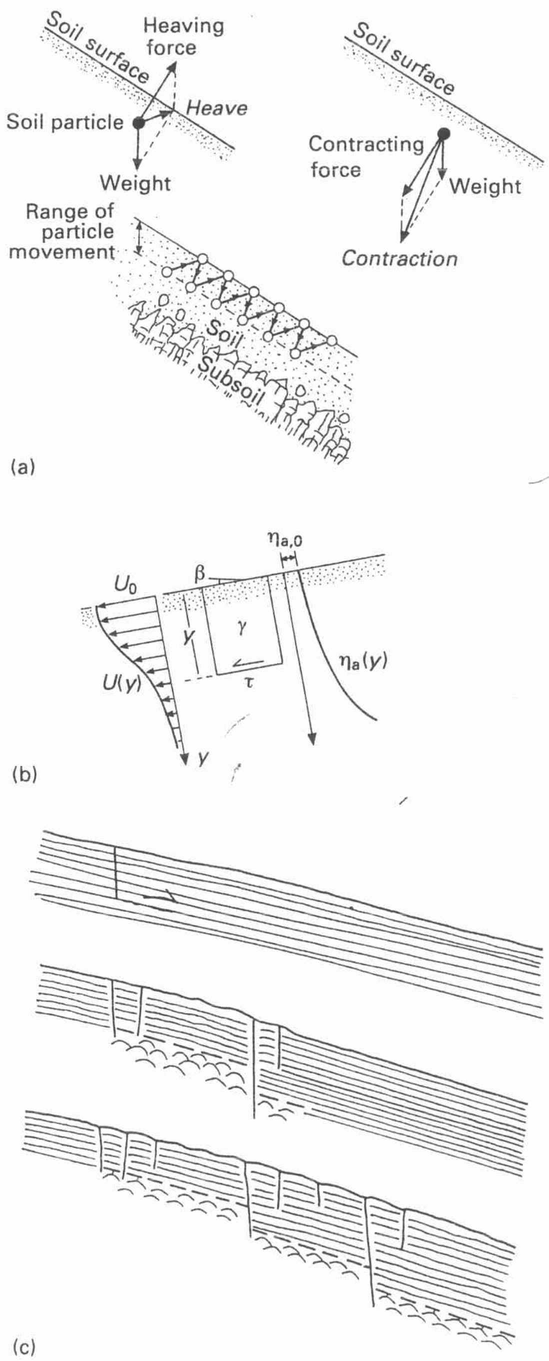

Fig. 8.4 Models for sediment creep on a gentle submarine slope. (a) Movement of soil particles during soil creep; (b) definition of terms for soil creep (see text for explanation); (c) progressive development of sediment creep along a 30–50 m subsurface decollement zone. (After Allen, 1985 and Stow, 1986.)

known. However, it is believed to be a widespread and very significant process in the deep sea.

At high ratios of shear stress to shear strength, creep deformation may accelerate rapidly to creep rupture and may thus act as a precursor to slide or slump failure.

8.2.4 Sliding and slumping

Sliding and slumping are more or less synonomous terms that describe downslope displacement of a semi-consolidated sediment mass along a basal shear plane while retaining some internal (bedding) coherence. Sliding emphasizes the lateral displacement along either simple *translational* or slightly *rotational* shear planes with little internal disturbance, whereas slumping emphasizes the internal disturbance and folded shear planes. These processes are very widespread on slopes of all gradients greater than about 0.5° and range in volume from less than 1 m^3 to over 100 km^3 and can be several hundreds of metres thick (Morgenstern, 1967; Saxov & Nieuwenhius, 1982). Embley (1980) claims that at least 40% of the continental rise off eastern North America is covered by a veneer of mass-flow deposits (slides and debrites).

Sediment instability on slopes is affected by numerous interacting variables (Schwarz, 1982; Lee, 1989) including: (1) the slope angle; (2) high rates of sedimentation, leading to high water content and low shear strength; (3) repeated cyclic stress, commonly caused by seismicity but also influenced by oceanographic factors such as currents and internal waves; (4) high primary productivity and/or bottom water anoxicity, both leading to high organic carbon content in the sediment; and (5) generation of gas in the sediment due to clathrate decomposition and organic matter decay.

Assessing sediment stability on slopes has generally used a static infinite slope model (Moore, 1961; Morgenstern, 1967) in which the lateral extent of the slope is much greater than the thickness of the sediment. This model expresses a safety factor, *SF*, as the ratio of the resisting force to the shear force, given by:

$$SF = \left[\frac{1-\Psi}{\rho_s g' Z \cos^2\beta}\right]\left[\frac{\tan\phi}{\tan\beta}\right], \qquad (8.2)$$

where Ψ is excess pore fluid pressure, *Z* is depth below the surface, ρ_s is sediment density, ρ is water density, g' is $g\int(\rho_s - \rho)/\rho_s$ in reduced gravitational constant, β is the slope angle, ϕ is the angle of internal friction.

It has been shown that the probability of failure is low for $SF > 1.3$, and failure is almost certain for $SF < 0.9$ (Athanasiou-Grivas, 1978). Hein and Gorsline (1981) concluded from their study of geotechnical characteristics of slope sediments in the Californian Continental Borderland that sedimentation rates in excess of 30 mg cm^{-2} $year^{-1}$ must be attained before slope failures become common.

A large slide on a gentle slope typically has the morphology shown in Fig. 8.5 (Lewis, 1971; Dingle, 1977). The head is characterized by tensional structures such as faults, slump scars and bed deficiency. Above the head area retrogressive slumping may have occurred, involving successive sediment failure and the upslope progradation of unstable slump scar surfaces. The main body of the slide mass can be relatively undisturbed or contain several distinct slump blocks, whereas the toe area displays compressional structures such as thrusting and overriding of beds.

The complexity of slide features on modern slopes has been amply demonstrated by recent studies (Lee, 1989; Barnes & Lewis, 1991; Simm *et al*, 1991), which clearly show the gradation that exists in nature between slide, debris flow and turbidity current processes and products.

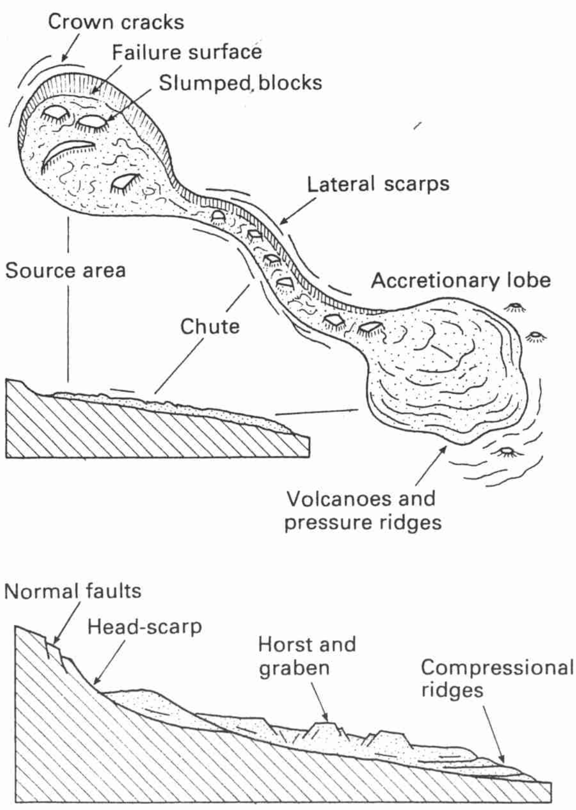

Fig. 8.5 Characteristics of sediment slides. (After Allen, 1985).

8.2.5 Debris flows

Debris flows are highly concentrated, highly viscous, sediment dispersions that possess a yield strength and display plastic flow behaviour (Johnson, 1970; Hampton, 1972). They are slurry-like or glacier-like, slow laminar flows that advance down slopes in excess of only 0.5°, either continuously or intermittently. They are best known from modern sub-aerial settings (Pierson, 1981; Takahashi, 1981; Johnson, 1984), where they are capable of carrying boulders up to 2.7×10^6 kg, may move at speeds of 20 m s^{-1} and have bulk densities in the range of $2\text{–}2.5 \times 10^3$ kg m^{-3}. Only a small amount (about 5%) of interstitial matrix (i.e. mud and water) is required to allow flow over even gentle slopes (Hampton, 1975, 1979).

Numerous recent surveys of marine slopes have shown the widespread importance of debris flows in moving large volumes of material, often many tens or hundreds of kilometres downslope. Catastrophic debris flows may transport enormous slabs up to about 2.3×10^9 kg (immersed weight, Marjanac, 1985).

Debris flows move when the critical yield strength is exceeded and deformation (flow) begins in a basal zone of highest shear stress. Here there is a complex region of sliding, rolling, bouncing and laminar flow. Higher in the flow, where shear stresses are less, the material may be rafted along as a semi-rigid plug. Deposition occurs by downward thickening of this plug until the entire mass freezes. Flow margin freezing may also occur and result in the construction of debris levees.

The motion of debris flows is perhaps even more difficult to model than that of slides. Lowe (1982) advocates a strictly cohesive model based on Bingham plastic behaviour, Johnson (1970) favoured either a Bingham-plastic or a Coulomb-viscous rheological model, whereas Takahashi (1981) proposed a 'dilatant-fluid' rheological model based entirely on dispersive pressure. Allen (1985) has used the Bingham-plastic model to derive a mathematical model in which flow velocity, U, is given by:

$$U = \frac{1}{\eta_a}\left[\frac{(\gamma - e)g \sin\beta}{4}(R^2 - r^2) - \tau_{yd}(R - r)\right], \quad (8.3)$$

where η_a is the apparent viscosity (Bingham viscosity), γ is the bulk density of the debris flow, e is the density of the fluid medium, β is the slope angle, R is the channel radius in which the debris flow moves, r is the radius of the rigid plug of debris flow, τ_{yd} is the plastic yield strength.

However, it appears most likely that natural debris flows display a wide range of rheological properties, being more or less cohesive-plastic, viscous-fluid and granular-collisional in behaviour (Shultz, 1984; Pickering *et al.*, 1989). The clast support mechanisms would also vary, including a combination of buoyancy, frictional strength, matrix strength, elevated pore pressures of the matrix, and dispersive pressure. Pickering *et al.* (1989) also discuss the possibility of some very large flows being turbulent in part.

The principal features of submarine debris flows include: (1) a head region or gathering area; (2) a channelized portion that may develop debris levees and raft large blocks in a central plug zone, and (3) a lobe/sheet depositional area. Commonly, the front of the flow forms a steep scarp up to 30 m or more in height, but on steeper slopes the flow is thinner, more rapid and has a lower elevation to the mud nose (Fig. 8.6). As debris flows advance downslope they load the underlying deposits and may induce secondary failure on the sea bed. They can also give rise to slumping where either the nose of the flow or the slope of the sea bed becomes oversteepened.

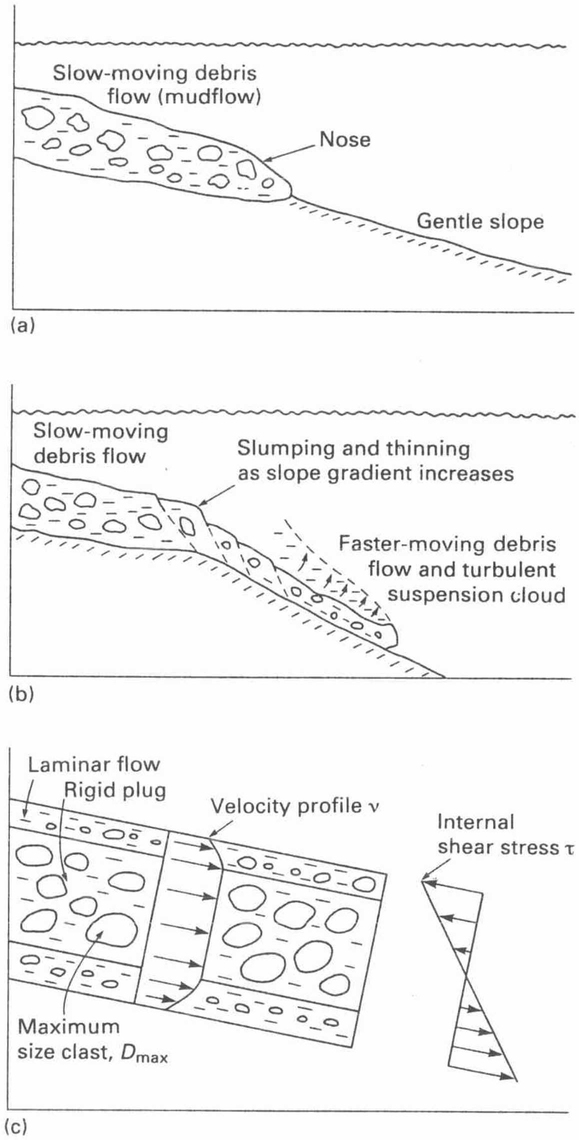

Fig. 8.6 Model and characteristics of sub-aqueous debris flows. Shear strength, $S = c + \sigma \tan \phi$; flow initiation, $\tau \geqslant S$. Steady flow, $\tau = S + \eta$; competence, $D_{max} = 8.8c/g(\rho_s - \rho_f)$. (After Stow, 1986.)

8.2.6 Grain flow, liquefied flow, fluidized flow

In an early classification scheme for sediment gravity flows (Middleton & Hampton, 1973; Middleton & Southard, 1984), four process end members were recognized: debris flows, liquefied flows (originally called fluidized flows), grain flows and turbidity currents. These were recognized as idealized, and it has become clear that the only sediment–gravity processes capable of long-distance transport over relatively gentle slopes are debris flows and turbidity currents. However, both these processes may involve or pass through stages of grain flow and liquefied/fluidized flow.

True grain flows are quasi-visco-elastic flows characterized by grain-to-grain collisions that result in a dispersive pressure support mechanism (Bagnold, 1954). They require slopes in excess of about 18° and so are probably a very localized process in the deep sea, perhaps occurring as small-scale sand avalanches in the heads of submarine canyons (Shepard & Dill, 1966). From an analysis of the mechanisms of grain flow, Lowe (1976) demonstrated a near-parabolic velocity profile with a thin surficial plug of non-shearing grains moving passively above an active shear plane. Lowe further concluded that sandy grain flows cannot be thicker than a few centimetres and so cannot be solely responsible for the deposition of thick massive sand beds.

Liquefied and fluidized flows are related processes that involve the collapse of a metastable fabric and partial or full grain support by upward-moving pore fluids. The grains become suspended and the sediment strength is reduced to zero. Loosely packed silt and sand are especially susceptible to fluidization, whereas gravel is usually too porous and in muds the cohesive forces resist fluidization (Lowe, 1975, 1979; Middleton & Hampton, 1976). Fluidized sand behaves like a fluid of high viscosity and can flow rapidly down slopes in excess of 2–3°. The excess pore fluid pressures dissipate quickly, from minutes to a few hours, depending on flow thickness and grain size. Deposition occurs through a short period of liquefied flow in which the grains settle rapidly and the flow freezes bottom to top.

8.2.7 Turbidity currents

Definitions and flow initiation

Turbidity currents are a type of density current or gravity current (Simpson, 1982) in which the denser fluid is a relatively dilute suspension of sediment. Many other types of density current exist in nature, including *overflows* such as plumes of fresh mud-laden water at river mouths, *underflows* in the atmosphere (sea-breeze fronts and dust storms), powder-snow avalanches, pyroclastic base-surges and *nuées ardentes* emanating from volcanic eruptions, and *vertical density flows* caused by plumes of volcanic ash falling through the atmosphere and oceans (Allen, 1985).

The turbidity current is the main type of sediment-driven underflow in the oceans, seas and lakes, the most important and perhaps best known of the resedimentation processes. Although much studied in the laboratory and theoretically, a full-sized prototype has never yet been observed in nature. The evidence for their occurrence comes from observations of density underflows in lakes, incipient, small, dilute turbidity currents in the heads of canyons, and the sudden, unexpected but sequential breaking of submarine telegraph cables (Heezen *et al.*, 1954; Krause *et al.*, 1970). From the almost ubiquitous occurrence of their characteristic deposits, turbidites, they are known to occur widely throughout the deep sea.

Depending on the manner in which the flow is initiated and on subsequent sediment supply, two main types of turbidity current can be identified: relatively short-lived *surge-type* flows, and relatively long-lived *steady-* or *uniform-type* flows. Flow initiation occurs in one of four main ways: (1) from the transformation of slumps or debris flows by mixing with seawater; (2) from sand-spillover, grain flows or rip-currents feeding sediments into the heads of submarine canyons; (3) by storm stirring of unconsolidated bottom sediments and the build-up of a concentrated shelf nepheloid layer; and (4) directly from suspended sediments delivered to the sea by rivers in flood or by glacial meltwaters.

Mathematical models

In reality, turbidity currents are non-uniform, unsteady, non-linear, free-boundary flows, that move by virtue of dispersed sediment, which may both be deposited during flow and eroded from the substrate over which the flow passes. With these characteristics, Allen (1985) has argued, it is not yet possible to construct a comprehensive theoretical model, although attempts have been made to explore certain aspects of turbidity flow under severe constraints. For 'uniform' flows (Fig. 8.7), Middleton (1966a) proposed a Chezy-type equation, in which the velocity of the body of the turbidity current, U_B, is given by:

$$U_B^2 = \left[\frac{8g}{(f_o + f_i)}\right]\left[\frac{\Delta\rho}{(\rho + \Delta\rho)}\right] d_B \tan\beta, \qquad (8.4)$$

where $\Delta\rho$ is the density difference between the flow and seawater, ρ is the density of seawater, d_B is the thickness of body, β is the slope angle, f_o is the dimensionless friction coefficient at the base of the flow, f_i is the dimensionless friction coefficient at the top of the flow.

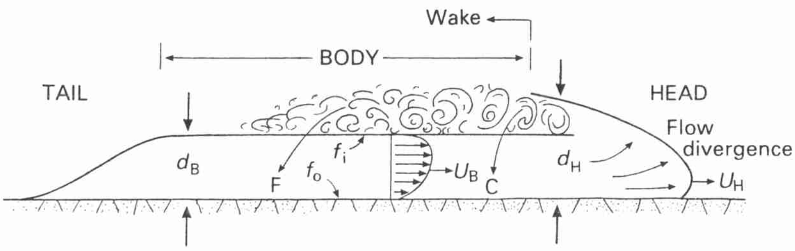

Fig. 8.7 Model and characteristics of uniform turbidity current. (After Pickering *et al.*, 1989.)

For the velocity of the head of the current, U_H, Middleton (1966b) gives:

$$U_H^2 = 0.56 g d_H \left[\frac{\Delta\rho}{(\rho + \Delta\rho)}\right]. \quad (8.5)$$

One problem with using Eq. 8.4 is lack of knowledge of the friction coefficients. Middleton and Southard (1984) suggest that for large flows ($f_o + f_i$) is likely to be about 0.01, and that the difference between f_o and f_i will vary considerably depending on whether the flow is super-critical or sub-critical (i.e. respectively with or without intense mixing at the upper interface).

Equation 8.5 indicates that the velocity of the head is independent of the slope angle and this is believed to be true for relatively gentle slopes (i.e. < 1.24°). For steeper slopes, from perhaps 2 to 10°, Hay (1983) has proposed a modified flow equation that includes a dependence on bottom slope. The ratio of head velocity to body velocity, U_H/U_B, is found from experimental work to be approximately unity for gentle slopes but less than 1.0 on steeper slopes. As coarse-grained material from the body enters the head there is a corresponding loss of fine suspension from intense mixing in the neck region and settling back into the top of the body flow. Thus an equilibrium is maintained and a lateral grading developed from a coarser suspension in the head to a finer suspension in the tail.

The slope also has a key effect on whether turbidity currents are sub-critical (Froude number < 1.0) or super-critical (Froude number > 1.0). For a reasonable friction factor, $f = 0.02$, Komar (1971) demonstrated that turbidity currents would be super-critical on slopes > 0.5°, which would commonly be the case on many basin slopes and upper fan settings. Where the slope gradient decreases in the base-of-slope region then transition of sub-critical flow occurs, probably involving a hydraulic jump with intense turbulence and flow homogenization.

Autosuspension and ignition

In all turbidity currents the sediment-support mechanism which keeps the sediment particles in suspension is provided primarily by the upward component of fluid turbulence, which is mainly sustained by friction at the boundary between the flow and both the floor and the ambient fluid. It has been argued that turbidity flow can be sustained in the form of autosuspension (Bagnold, 1962). Autosuspension is a process of flow self-maintenance (Southard & Mackintosh, 1981) whereby a state of dynamic equilibrium is achieved in which (1) the excess density of the suspended sediment propels the flow; (2) the flow generates friction and fluid turbulence; and (3) the turbulence keeps the sediment particles in suspension, and so on (Fig. 8.8). All that is needed to keep the loop intact is that the loss of energy by friction be compensated for by a gain in gravitational energy as the flow travels downslope. In this theoretical model it is possible for a turbidity current to travel over long distances without appreciable erosion or deposition as long as the slope remains constant.

Later work (Southard & Mackintosh, 1981; Middleton & Southard, 1984) has shown that true autosuspension is not always achieved and that as energy is lost from the system so some of the suspended load settles through the flow and is deposited. Pantin (1979) introduced an efficiency factor, e, into the autosuspension model, such that:

$$e\beta U_s > w, \quad (8.6)$$

where β is the slope angle, U_s is the transport velocity of suspended sediment, w is the grain settling velocity. Pantin (1979) showed that flow density is the main determinant on whether autosuspension will occur. Below a critical density a turbidity current will subside and deposit, whereas above this value the

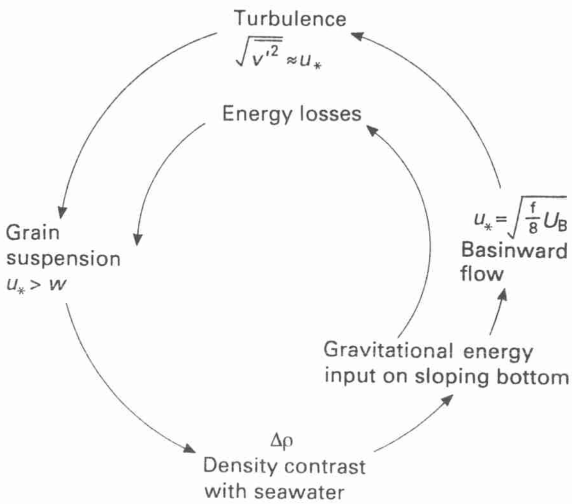

Fig. 8.8 Conceptual diagram to explain autosuspension. If gravitational energy input = energy losses, the flow will be self maintaining, and grains with settling velocity w will be maintained in suspension by vertical velocity fluctuations of average stregnth $\sqrt{v'^2}$ approximated by u_*. (Middleton 1976). u_* is related to body velocity, U_B, through friction factor, f. See text for explanation. (After Pickering *et al.*, 1989.)

flow will 'explode', increasing in density and velocity and achieve autosuspension. This is known as flow *ignition* (Fukushima *et al.*, 1985).

Flow characteristics

Observations of atmospheric and pyroclastic density flows together with experiments on sub-aqueous density suspensions have shown that turbidity currents develop a characteristic longitudinal anatomy of head, neck, body and tail (Fig. 8.7) (Middleton, 1966a; Middleton & Hampton, 1976; Allen, 1985). The head of a turbidity current has a characteristic shape and flow pattern. In plan view, the head appears lobate with local divergencies of flow direction and a spanwise arrangement of regularly spaced lobes and clefts (Simpson, 1969, 1972; Allen, 1971). Inside the head a forward and upward sweeping, circulatory flow pattern exists. The coarsest grains tend to become concentrated in the head. The body is the part behind the head where the flow is almost uniform in thickness. Deposition may take place from the body while the head still erodes. The tail is the part where the flow thins rapidly and becomes very dilute. Mixing between the flow and the ambient fluid produces a dilute entrained layer. On slopes greater than 1.24° the head is thicker than the body, whereas on lesser slopes the body is thicker than the head (Komar, 1971). This is important for the type of sediment overflow in channelized environments. Mixing of the flow with water, loss of sediment by deposition and by flow separation in the neck will slacken and eventually stop the turbidity current. In an average turbidity current most coarse sediment will be deposited in a timespan of hours, though complete settling of the fine-grained tail may take a week (Kuenen, 1967).

Turbidity currents in the oceans are several orders of magnitude larger than those produced in laboratory flumes, so that the extent to which experimental results can be applied to turbidity currents in nature is somewhat problematic. The closest we have come to high density currents in nature is noting the occurrence of sequential breakages of submarine cables. The classic example is the Grand Banks earthquake of 1929 that triggered an enormous slump and an ensuing turbidity current that travelled downslope for hundreds of kilometres on to the Sohm Abyssal Plain (Heezen & Ewing, 1952; Piper & Normark, 1982). The maximum velocity attained by this current was some 70 km h^{-1} (25 m s^{-1}) (Menard, 1964). Other well-documented examples have occurred off the coast of Algeria, from the canyon systems off the mouths of the Congo and Magdalena rivers and in the western New Britain Trench (see summary by Heezen & Hollister, 1971). Estimated velocities were again of the order of tens of kilometres per hour.

Some idea of the width and thickness of turbidity currents and the distances they travel can be deduced from the resulting depositional topography. The natural levees of submarine channels are believed to be produced from the overflow of channelized turbidity currents. Such currents must therefore be up to several kilometres wide and several hundreds of metres thick (Komar, 1969; Nelson & Kulm, 1973; Stow & Bowen, 1980). The length of deep-sea channels and of the flat expanses of abyssal plains both indicate that turbidity currents can travel as far as 4000–5000 km (Curray & Moore, 1971; Chough & Hesse, 1976; Piper *et al.* 1984; Stow *et al.*, 1990).

Various attempts have been made to estimate the physical features of low-density turbidity currents (Shepard *et al.*, 1977, 1979; Stow & Bowen, 1980; Bowen *et al.*, 1984) (Table 8.3). They vary in thickness from a few metres to channel-full flows over 800 m thick and have velocities in the range 10–50 cm s^{-1}.

Flow lofting

Turbidity currents generally carry warm, less dense water (normal marine or brackish) into denser deep-sea medium by virtue of an excess density due to suspended sediment. However, after sufficient particles have been deposited, the current will become progressively more buoyant, cease its lateral motion and ascend to form a plume in a process known as *lift-off* or *flow lofting* (Sparks *et al.*, 1993).

Sparks *et al.* (1992) discuss the concept of such sediment-laden gravity currents that come to display a reversing buoyancy from theoretical and experimental evidence. They postulate a vertical mixing of the dilute suspension and warmer water into the overlying weakly stratified ocean. They also suggest that the fine sediment from the lofted fluid may become much more widely dispersed than the main turbidity current deposit.

Arguing from observations made on sediments recovered from the distal Bengal Fan in the central Indian Ocean, Stow and Wetzel (1990) propose a very similar process, which they believe is commonplace in distal turbidite settings. They suggest that the 'dying' turbidity current discharges its suspension into the water column, up to hundreds or more than a thousand metres above the ocean floor. Further

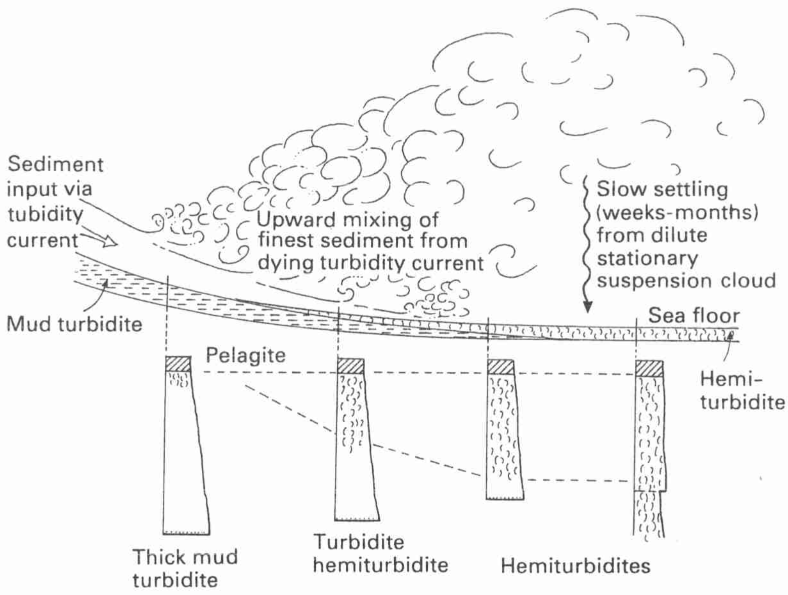

Fig. 8.9 Model for flow lofting and hemiturbidite deposition. (After Stow & Wetzel, 1990.)

material is added to this suspension cloud as the tail of the turbidity current arrives in the area over a period of, perhaps, a few days to a week or more. Material from this cloud then settles very slowly to the sea floor both above and beyond the distal feather edge of the muddy turbidite deposited by the original current. On the basis of continuous bioturbidation throughout, Stow and Wetzel (1990) propose a time scale of a few weeks to many months for deposition of a 1-m thick unit. They call these deposits *hemiturbidites* (Fig. 8.9).

8.3 Bottom current processes

8.3.1 Introduction

The second main group of processes that operate in the deep sea, actively eroding, transporting and depositing sediment, are collectively known as bottom currents (or 'normal bottom currents' — Stow, 1986). These include all types of deep current that are *not* normally driven by sediment suspensions but that result from normal oceanographic forces such as winds, tides, waves and thermohaline circulation. The main types and characteristics of these currents are shown in Table 8.3.

The ocean waters, shallow and deep, can be compartmentalized into different water masses, each having distinctive temperature/salinity (T–S) characteristics. A profile across the North Atlantic Ocean (Fig. 8.10) shows the layered distribution of these water masses. More than 75% of the world ocean and almost all of the water below 1000 m has T–S characteristics within the relatively narrow limits of $-1°C$–$5°C$ and 34.4–35%. Only the near-surface water can be significantly warmer and marginal seas (e.g. Red Sea, Mediterranean Sea) more saline.

In this section, we are mainly concerned with the origin, nature and movement of these deep water masses and with how they become intensified into discrete currents.

8.3.2 Bottom (contour) currents

Origin and intensification

Deep ocean bottom water is formed by the cooling and sinking of surface water at high latitudes (Gill, 1973; Killworth, 1973) and the deep, slow thermohaline circulation of these polar water masses throughout the world's oceans (Neuman, 1968). Highly saline but warm water also flows out of the Mediterranean Sea as an intermediate-level water mass.

Antarctic Bottom Water (AABW), the densest and deepest water in the oceans, forms in the region of the coast-hugging westward-directed surface Polar Current, with localized areas of major generation, such as the Weddell Sea, where the formation of sea ice, at about 1.9°C increases the salinity of the water remaining. This water then runs down the continental

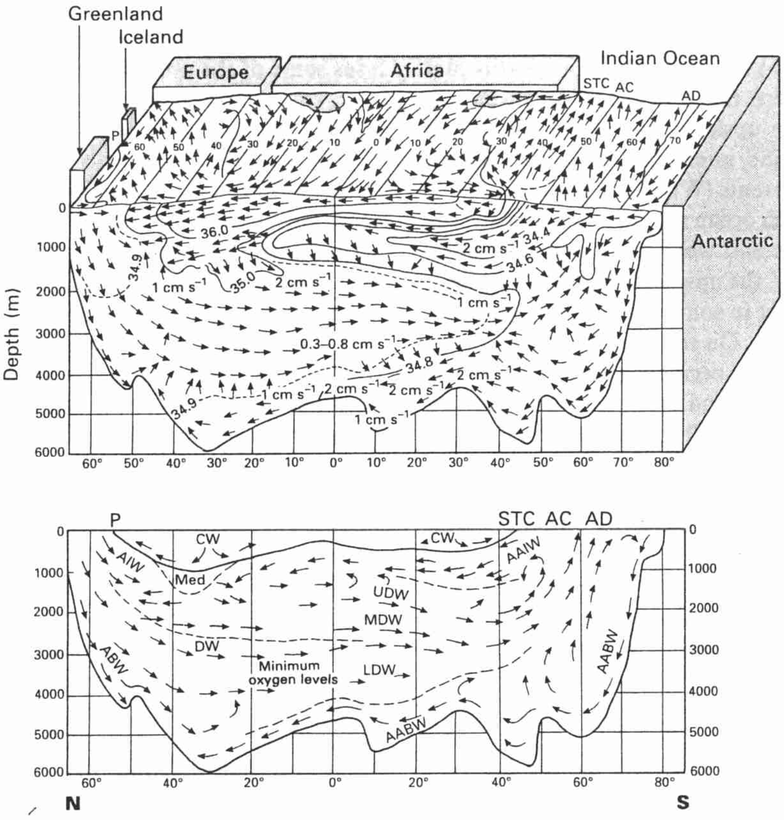

ABW : Arctic bottom water
AABW: Antarctic bottom water
AAIW: Antarctic intermediate water
AIW : Arctic intermediate water
CW : Central water
DW : Deep Atlantic water
UDW : Upper deep water
MDW : Middle deep water
LDW : Lower deep water

Med : Water from the Mediterranean
: Regions of upwelling
AC : Antarctic convergence
AD : Antarctic divergence
STC : Subtropical convergence
P : Arctic polar front
---- : Minimum oxygen levels

Fig. 8.10 Bottom water masses in the North Atlantic Ocean.

slope, circulates eastwards around the Antarctic continent, perhaps several times, and then flows northwards into the Atlantic, Indian and Pacific Oceans. It can still be recognized, although considerably warmer, in the central and northern Atlantic Ocean where it mixes with and contributes to the North Atlantic Deep Water (NADW). AABW is also the main source of Pacific and Indian Ocean Common Water (PIOCW).

A major source of NADW appears to be the sub-polar gyre in the Norwegian and Greenland Seas, although it remains partly trapped by an irregular topographic barrier known as the Scotland–Iceland–Greenland Ridge. Once the Norwegian–Greenland Seas basin is filled with this cold, dense water mass then intermittent overflow to the south occurs through narrow channels cutting across the Ridge. Overlying water is entrained by turbulent shearing and helps impart distinctive characteristics to a NE Atlantic Deep Water (NEADW) and a NW Atlantic Deep Water (NWADW) mass. NWADW mixes with Labrador Sea Water (LSW), which is formed by surface cooling in the Labrador Sea. NEADW in part moves south within the eastern Atlantic basin and part crosses the Mid-Atlantic Ridge to mix with and partly overlie NWADW.

These slowly moving water masses are affected by the Coriolis Force, due to the Earth's spin, which deflects moving bodies to the right in the northern hemisphere, to the left in the southern hemisphere and is zero at the equator. The result is that deep-water flows are banked up against the continental slopes on the western margins of the ocean basins, are unable to move upslope against gravity and so become restricted and intensified, forming Western Boundary Undercurrents (WBUC).

Deep water in each ocean spreads slowly eastwards from these WBUCs and wells up through the main thermocline. Mostly, the upwelling is a slow, uniform upward diffusion, but in some coastal and equatorial regions it is enhanced. On reaching the upper layers of the oceans, the water becomes part of the normal wind-driven circulation and eventually finds its way back to the polar regions. The generalized pattern of deep circulation is shown in Fig. 8.11 (Stow & Lovell, 1979), which agrees well with that modelled by Stommel (1957) and predicted by Stommel and Aarons (1960b).

Bottom currents are also locally intensified by flow restriction through narrow passages in the deep sea, for example in flowing through Fracture Zone gaps in the Mid-Ocean Ridge system.

Mathematical models

The complexity of models needed to describe deep-sea circulation and its coupling with the general oceanic circulation is beyond the scope of this chapter, and better left to more specific texts on dynamic oceanography (e.g. Tolmazin, 1985). Nowell and Hollister (1985) outline the essence of an Ekman layer–sediment transport model as a prelude to the High Energy Benthic Boundary Layer Experiment (HEBBLE, see later), and McLean (1985) analyses some of the preliminary results.

Flow characteristics

Whereas much of the deep-sea floor is swept by very slow currents (< 2 cm s^{-1}), the western boundary currents commonly attain velocities of 10–20 cm s^{-1} and these may be greater than 100 cm s^{-1} where the flow is particularly restricted (Stow & Lovell, 1979; McCave & Tucholke, 1986).

Although these bottom currents are more or less continuous and sufficiently competent in parts of the ocean to erode, transport and deposit sediment, they are also highly variable in both velocity and direction (Luyten, 1977; Richardson *et al.*, 1981; Nowell & Hollister, 1985). Large-scale eddies peel off and move at right angles to the main flow, and the average velocity decreases from the core to the margins of the current. Both seasonal (Shor *et al.*, 1980) and tidal (McCave *et al.*, 1980) periodicities have been recorded, and current reversals are common. The currents vary from a few kilometres to tens of kilometres in width and can flow at different levels within the water column depending on the relative densities of adjacent water masses.

Well-developed nepheloid layers (Fig. 8.12), or turbid bottom waters with marked concentrations of suspended matter, are commonly associated with the higher velocity bottom currents in many parts of the ocean basins (Eittreim *et al.*, 1976; Biscaye & Eittreim, 1977). These currents appear to maintain fine (average size 12 μm) particles in suspension by

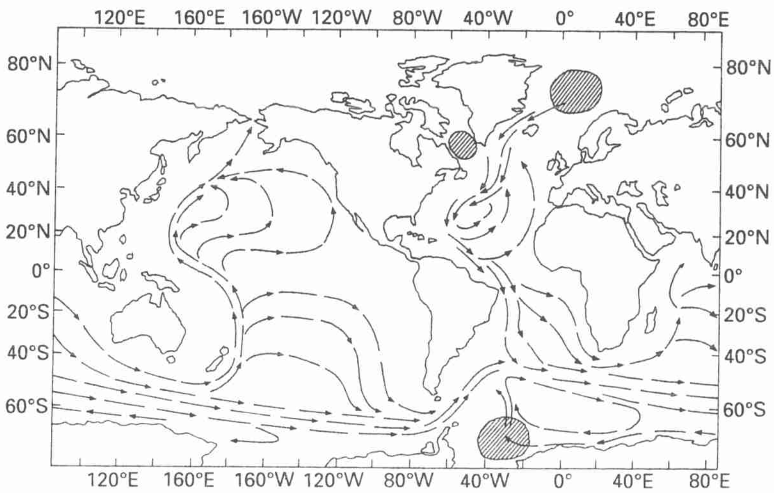

Fig. 8.11 Global pattern of abyssal circulation. (After Pickering *et al.*, 1989).

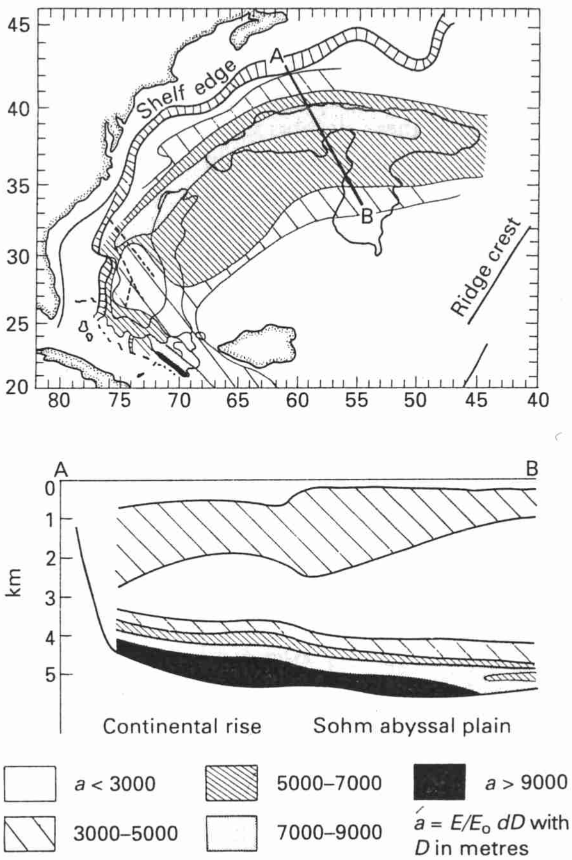

Fig. 8.12 Nepheloid layers in the NW Atlantic Ocean. (After Stow, 1986.)

turbulent eddy diffusion for a residence period of about 1 year (Eittreim & Ewing, 1972). Concentrations of deep-sea nepheloid layers are extremely low (0.01–0.3 mg l^{-1}, McCave & Swift, 1976) and their thicknesses vary from less than 100 m to over 1000 m.

Although bottom currents are clearly efficient agents of particle transport and redistribution, both terrigenous and biogenic, and play a major role in shaping deep-sea morphology (see later), for many years we have had no very good understanding of the exact nature of erosional and depositional processes by bottom currents. Whereas, the velocities commonly recorded by current-metre measurements were adequate to transport fine-grained material, they were insufficient to effect marked erosion of very cohesive deep-sea muds. There has also been a debate centred around the role and extent of reworking of silts and sands by bottom currents compared with transport and deposition. However the result of the HEBBLE programme, on the lower continental rise off Nova Scotia (Hollister & McCave, 1984), and of several detailed studies of the nepheloid layer (McCave, 1986) have, more recently, shed much light on this whole problem.

We know that the hydrodynamic processes acting on the deep-sea floor are the result of an interplay of deep-sea circulation and surface current activity, which is mainly controlled by atmospheric conditions. What the HEBBLE work clearly demonstrated is that temporary very high surface energy conditions may propagate downward and induce high energy over the deep-sea floor. Very high surface kinetic energy in the oceans, as shown by maximum variability in the level of the sea surface (Richardson, 1983; Cheney *et al.*, 1983), is only observed in relatively few areas, such as in the NW Atlantic along the eastern US margin, or in the SW Atlantic along the Argentine margin. These are also areas of significant contourite sedimentation.

The variation of bottom kinetic energy conditions in the HEBBLE area results in an alternation of short (days to weeks) episodes of erosion associated with high velocity currents, and longer periods (weeks to months) of deposition associated with lower velocity. Episodes of high current velocity, called 'benthic', 'abyssal' or 'deep-sea' storms (Gardner & Sullivan, 1981; Hollister & McCave, 1984), correspond to high surface kinetic energy, due to local very low atmospheric pressure. During these episodes, a large volume of material is resuspended and thus contributes to a very high density nepheloid layer. This material may then be transported over long distances in the Western Boundary Undercurrent before eventual deposition. Between abyssal storm events, the current velocities are much lower and very high sedimentation rates occur (up to 1.4 cm $month^{-1}$), over these short time periods. However, the net sedimentation rate at the scale of Holocene deposits on this part of the continental rise, is very low (5.5 cm per 10^3 years) as a result of the very frequent and active erosional episodes (estimated annual deposition/preservation ratio of 3100). At a greater geological scale (Neogene), similar rates of deposition (2–10 cm per 10^3 years) are observed on the giant contourite drifts in the North Atlantic Ocean.

Resuspension of sea-floor sediments is not the only process feeding the nepheloid layer and hence bottom-current transport. Several other processes may be involved including: (1) inputs of terrigenous particles from the adjacent margins by turbidity currents; (2) advection along isopycnal surfaces via suspension cascading or some other hemipelagic process; (3) direct settling of biogenic pelagic particles and pellets; (4) resuspension of particles by the burrowing activity of benthic organisms. Whatever the origin of the particles, it appears that there is a close relationship been high turbidity nepheloid layers and active bottom-current transport, including both erosion and deposition.

8.3.3 Major surface currents

The very large wind-driven current systems developed in the surface layers of the oceans can also have a direct effect even at very great depths (several kilometres). This is true of the deep Gulf Stream gyres of the North Atlantic (McCave & Tucholke, 1986), the deep Kuroshio Current off Japan and the Antarctic Circumpolar Current driven by the West Wind Drift.

8.3.4 Internal waves and tides

Surface waves and tides are some of the most important physical processes affecting sediments and biota in shallow water. As the sea is clearly a heterogeneous body, undulation swells or internal waves can also form between sub-surface water layers of varying density in the upper few hundreds of metres, most notably at the thermocline (Lafond, 1962). Such internal waves are very widespread and vary considerably in amplitude and periodicity. They may exceed surface waves in amplitude, although their speed of progression is usually slow (5–300 cm s^{-1}). Similar large-scale oscillations at density discontinuities have been shown to have a tidal period and are known as internal tides (Rattay, 1960).

The breaking and turbulent eddies caused by internal waves and the velocities attained by both internal waves and tides probably cause significant sediment stirring and erosion at the shelf break, on the tops of seamounts or in relatively shallow slope and shelf-basins (Shepard, 1973b). They are also thought to contribute to up-and-down canyon currents (Shepard *et al.*, 1979).

8.3.5 Canyon currents

Whenever current metres have been placed in deep-sea channels or canyons, originally with the intention of measuring turbidity current flow, it has been found that semi-permanent currents are everywhere present, even at depths in excess of 4 km (Shepard *et al.*, 1979). Generally, however, these currents alternate directions, flowing both up and down canyon with periodicities ranging from 15 min to 24 h and with velocities commonly up to 30 cm s^{-1} (Fig. 8.13). A tidal periodicity seems most usual in the deeper parts, but a higher frequency of flow reversal normally occurs in the head region. Other flow periods and directions have also been recorded, probably related to internal waves, surface currents, storm surges or cold-water cascading currents.

In some cases, following major storm periods

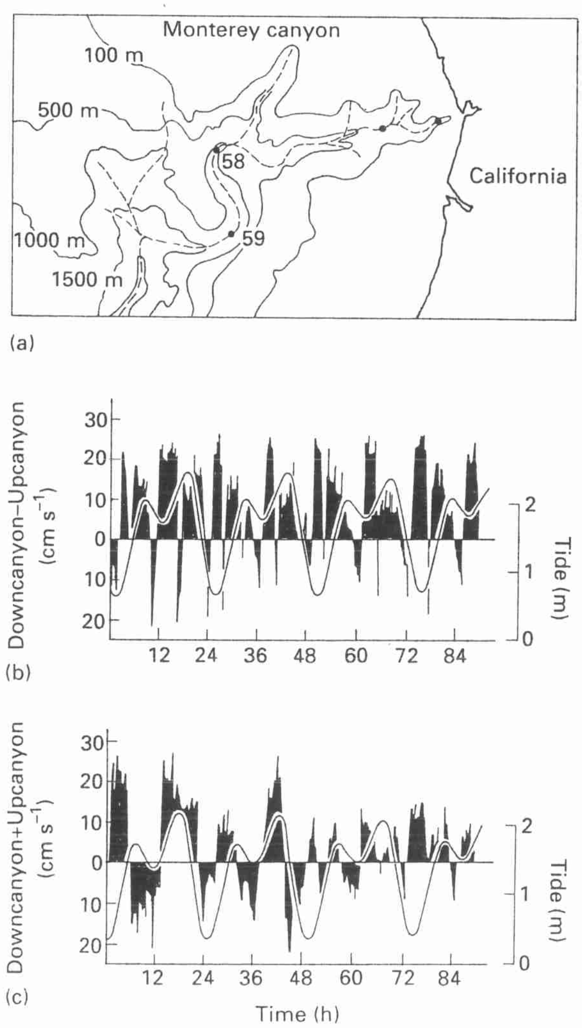

Fig. 8.13 Canyon currents within Monterey Canyon, off Western California. (a), Location. (b) Station 58, depth 1061 m. (c) Station 59, depth 1445 m. (After Stow, 1986.)

leading to the build up of water in the shallow shelf regions near canyon heads, prolonged downcanyon flows can develop attaining speeds of 50–100 cm s^{-1} lasting for several days. These are probably true low-density turbidity currents and not equivalent to the more common non-turbid canyon currents.

From the measured frequency and velocity of canyon currents it is clear that they have considerable effect on the winnowing, entrainment and movement of sediment, the moulding of canyon and channel morphologies and on keeping canyon floors generally free from pelagic or hemipelagic sedimentation.

8.4 Pelagic and hemipelagic processes

8.4.1 Introduction

Slow vertical settling of microscopic biogenic and non-biogenic particles through the water column, in the absence of significant effects of other processes at any depth within the open oceans, is generally referred to as *pelagic settling*. It is less important for clastic than for biogenic sediments as the materials involved are largely the tests of calcareous and siliceous planktonic organisms and their associated organic matter which has been biosynthesized in the surface layers of the oceans. These form the pelagic deposits of the deep sea (Jenkyns, 1986).

In many areas of the deep sea, particularly on slopes and in basins close to land, terrigenous elements (clays, quartz, feldspar, volcanic dust and other minerals) with a high proportion of silt-sized grains can form a significant part of the settling material and hence of the resulting *hemipelagic* deposit. Such materials are transported by surface currents, winds and floating ice and mix with pelagic biogenic components during settling (Stow, 1985).

8.4.2 Vertical settling of pelagic material

A simple way to model pelagic settling is to consider the free fall velocity, V_g, of a perfect sphere through the water column:

$$V_g = \frac{gd^2(\sigma - \rho)}{18\mu}, \quad (8.7)$$

where g is the acceleration due to gravity, d is the particle diameter, σ is the particle density, ρ is the fluid density, μ is the fluid viscosity.

This is known as Stokes' Law and yields fall velocities of the order of 10^{-4}–10^{-6} m s^{-1} for the finest silt- and clay-sized particles.

However, in nature, a number of factors mitigate against this ideal situation (Allen, 1985). Firstly, most particles are not spherical and many, including platy clays and elaborate siliceous or calcareous tests, are very far indeed from being spherical. Experimental results show a combination of tumbles, steady fall and oscillations for the settling behaviour of solitary discs in a stagnant fluid (Allen, 1985). Other work has measured differential fall velocities for a range of planktonic microfossils. Secondly, numerous observations of suspended sediment in the open oceans have revealed that particles very rarely settle in isolation. Instead, physical mechanisms of flocculation and biogenic processes of pelletization ensure that most material settles much more rapidly (10^{-2}–10^{-3} m s^{-1}) as flocs or pellets. Thirdly, falling particles are subjected to progressive dissolution of calcareous and siliceous tests (particularly below the Carbonate Compensation Depth, CCD), oxidation of organic matter and lateral transport by bottom currents, turbidity currents or other slow advection processes.

8.4.3 Settling and horizontal advection

Somewhere between vertical pelagic settling and low-density turbidity currents is a range of overlapping mechanisms that can conveniently be called *hemipelagic processes*. The materials involved are an admixture of terrigenous and primary biogenic particles (Jenkyns, 1986). Deposition is by slow settling, typically coupled with a component of current-induced lateral advection of suspended sediment in mid- or bottom-water nepheloid layers. This may involve suspension cascading, lutite flows, up and down canyon currents and very thin turbid-layer flows (McCave, 1972; Drake *et al.*, 1978; Stow, 1985) (Fig. 8.14).

8.5. Sediment nature and distribution

8.5.1 Introduction

Our main discussion thus far has concentrated on the nature of long-distance transport mechanisms into and within the deep sea. However, the character of the sediments deposited depends partly on these processes but partly also on the final mode of deposition and early postdepositional deformation.

In this section, then, we focus on the nature of deep-sea sediments, both modern and ancient, and what we can thereby learn of the final depositional

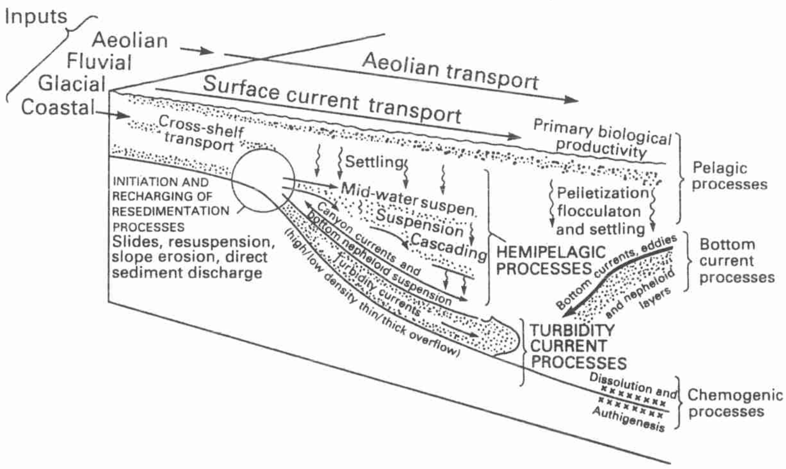

Fig. 8.14 Processes of fine-grained sedimentation in the deep sea indicating the range of processes contributing to hemipelagic deposition. (After Stow, 1985.)

processes involved. There have been many hundreds of research papers (and books) describing deep-sea sediments of every age and depositional setting from around the world. A synthesis of these data into a series of facies models seems the most useful approach to take here.

The analysis of sedimentary structures in both core and outcrop sections allows inference about the processes that caused them. However, only recently have we been able to observe directly and systematically the present day deep-sea sediment surface and bedforms from submersible dives and deep-tow near-bottom surveys. We begin our discussion with some of these observations, before considering how they may be preserved in ancient successions.

8.5.2 Bedforms and other sea-floor features

Mass wasting on slopes

All slopes surrounding deeper water basins, whether they are shelf, slope or oceanic in nature, are subject to mass wasting and show, to a greater or lesser degree, surface features that reflect these processes. The main characteristic of such slopes, particularly those that are relatively steep (> 5°), tectonically active and/or with a thick unstable sediment cover, is a generally irregular surface topography (Prior & Suhayda, 1979a; Hill, 1984). This is made up of: (1) erosional features such as slide, slump and debris flow scars, grooves and depressions formed by falling and passing olistoliths, and scour marks caused by high energy sediment gravity flows; and (2) depositional masses from rockfalls, slides, slumps and debris flows, chaotic rafted blocks, or slow sediment creep rucking the surface into semi-regular wrinkles or 'waves'. None of these is a true bedform shaped by fluid flow, but they are nevertheless very characteristic sediment surface forms caused by mass wasting (Fig. 8.15).

Turbidity current bedforms

A broad range of bedforms may be constructed on the sea floor during the passage of turbidity currents. In deep-sea channels covered with gravels and pebbly sands, deposited and moved by high concentration turbidity currents and associated sediment gravity flows, large-scale asymmetric gravel waves (wavelength 30–70 m, amplitude 5–10 m) and symmetrical macrodunes (wave length *c.* 300 m, amplitude 2–5 m) have recently been described (Hughes *et al.*, 1990). Earlier observations have rarely reported such regular gravel bedforms but have recorded more irregular or bar-like gravel lenses (Malinverno *et al.*, 1988). These have been inferred previously from studies of ancient series (Hein, 1982).

A new generation of deep-tow instrument packages is now being used to make very detailed observations of sea-floor features from, for example, channels on the Monterey Fan in the east Pacific. Towed Ocean Bottom Instrument (TOBI) data have revealed lenticular to irregularly-shaped channel bars, wave and dune fields, erosional steps transverse to the channel axis, and trains of roughly circular scours or pock marks oriented at an acute angle to the channel in overbank deposits (Fig. 8.16) (D. Masson personal communication).

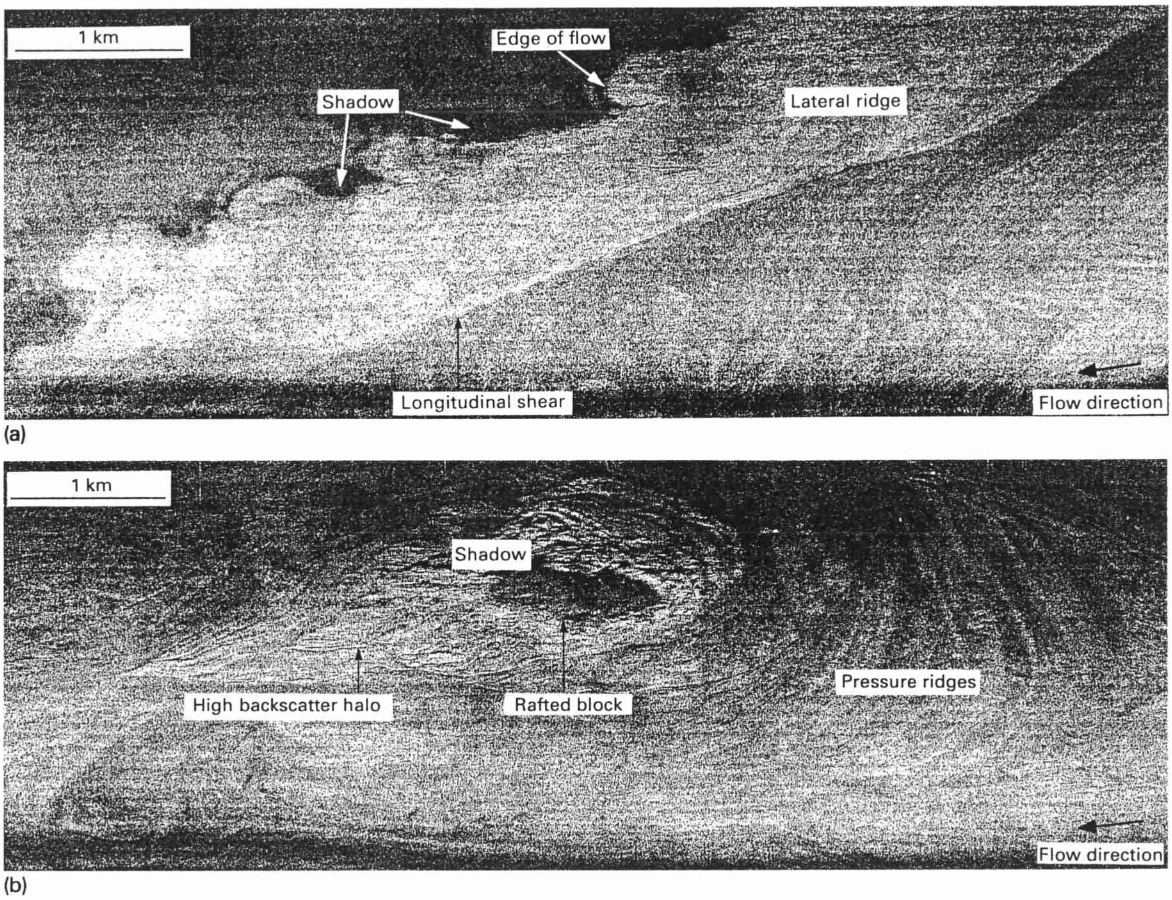

Fig. 8.15 Deep-towed 30 kHz sidescan sonograph (TOBI image) from the Saharan Debris Flow deposit in the northeast Atlantic. (a) Edge of debris flow deposit (lobate); (b) rafted block within debris flow deposit. (From Masson *et al.*, 1993.)

In some areas, channel levees are covered by regular large-scale sediment waves that typically show an upslope (up-current) migration when examined with high-resolution seismic profiling (Damuth, 1975; Normark *et al.*, 1980). These sediment waves typically show wave lengths of 0.5–2 km, amplitudes of 10–40 m, and are constructed in fine-grained muds and silty muds. Normark *et al.* (1980) considered them to be some kind of stationary wave or giant antidune bedform beneath a large low-concentration turbidity current that overtopped the confining bank on the outside of a channel meander. They noted a general decrease in amplitude and increase in wave length away from the channel.

Smaller-scale bedforms, such as dunes, ripples, lineated and smoothed surfaces, have been variously noted from beneath and presumed turbidity current pathways mainly from sea-bottom photographic surveys (e.g. Heezen & Hollister, 1971).

The erosional behaviour of turbidity currents is also well-known from longitudinal furrows and grooves as well as horse-show shaped flute marks scoured into soft substrates. Large and very large scale erosive features, megaflutes and giant flutes, have been described by Normark *et al.* (1979) from the Navy Fan and by Shor *et al.* (1990) from the Laurentian Fan (Fig. 8.16). Megaflutes may be 5–30 m across and 1–2 m deep, whereas the giant scour recently observed in the latter example is over 1 km long and 1 km wide at the flared end and up to 100 m deep near the apex.

Shor *et al.* (1990) also described smaller closed depressions that are 10–20 m deep and occur with regular spacing of 1.5–3 km along valley floor channels. These they believe are analogous to 'pools' developed on bedrock river floors.

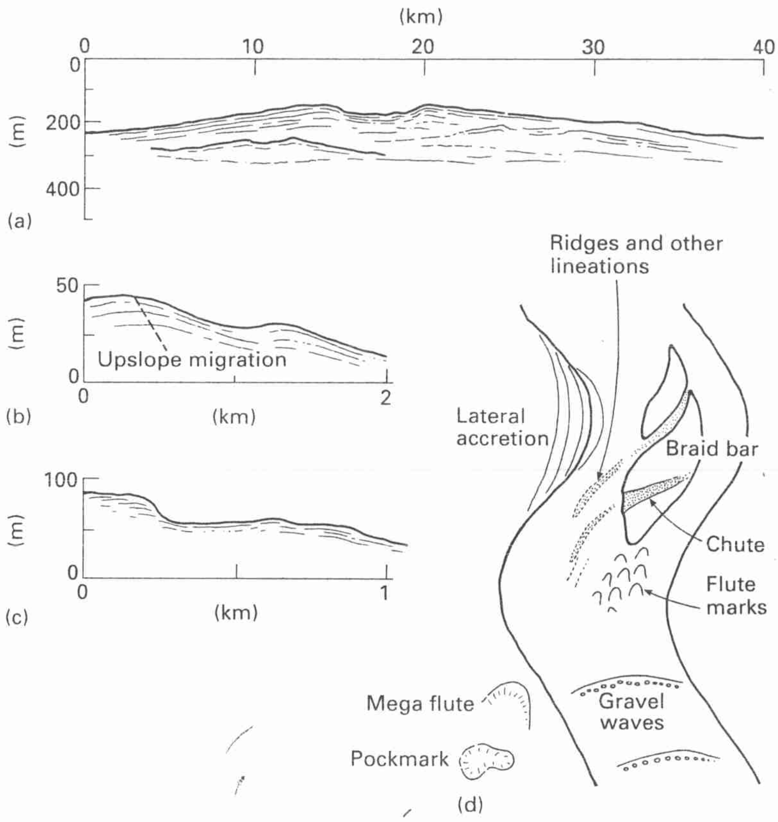

Fig. 8.16 Turbidity-current bedforms related to channel and non-channel/levee areas. Line drawings from seismic reflection profiles showing : (a) mid-fan channel-levee complex; (b) upslope migration of sediment waves on back side of levee; (c) longitudinal section of large-scale scour or megaflute; (d) schematic plan of portion of sinuous channel (approx. 1 km wide).

Bottom current bedforms

Bedforms controlled by bottom (contour) currents have been described in detail by many authors (Heezen & Hollister, 1971; Allen, 1982; Stow, 1982; Nowell & Hollister, 1985; McCave & Tucholke, 1986 among others; see also Stow & Faugeres, 1993). They occur at a range of scales from large sediment waves and erosional furrows to smaller scale dunes, ripples, lineation, scour and tail marks, etc. (Fig. 8.17). Bedform assemblages have been related to bottom-current intensity (Hollister & McCave, 1984), although the exact processes of formation still remain questionable for some of them, especially for giant sediment waves.

According to different authors working in different areas, sediment waves (Fig. 8.18) may be parallel, perpendicular or at an angle to current flow; they may propagate downstream or upstream, and if they are formed on a gentle slope, they can migrate downslope or upslope (Hollister *et al.*, 1974; Asquith, 1979; Lonsdale & Hollister, 1979; Embley *et al.*, 1980; Kolla *et al.*, 1980; Flood & Shor, 1988). Furthermore, these sediment waves are similar in dimensions and morphology to the sediment waves formed by turbidity currents outlined in the previous section (Normark *et al.*, 1980). The problem of a contour current or turbidity current origin for sediment waves is highlighted by examples from the Tyrrhenian Sea cited by Mariani *et al.* (1993).

Other sea-floor features

The deep-sea floor is moulded and modified by many other processes, which we do not have space to discuss further in this chapter. These include: (1) various types of wet-sediment injections (mud diapirs, volcanoes and ridges) that are particularly characteristic of active margin slopes and slope basins (Jones & Preston, 1987; Pickering *et al.*, 1989); (2) pock marks and other soft-sediment disturbances caused by shallow gas release, common beneath areas of active upwelling and high biogenic productivity (Summerhayes, 1992); (2) bottom relief and sediment drape caused by neotectonic fault activity (e.g. Pickering, *et al.* 1989; Redbourn *et al.*, 1993); and (4) iceberg scour marks and dropstone depressions on high latitude slope systems (Dowdeswell & Scourse, 1990).

8.5.3 Facies models and their hydrodynamic interpretation

Introduction

Each of the various processes discussed in Sections 8.2, 8.3 and 8.4 above gives rise to a characteristic deposit. These can be described in terms of a series of facies models (Figs. 8.19–21) which show the standard sequence of structures and other sedimentary features attributed to a particular process.

Slumps, slides and debrites

Slumps and slides occur at all scales and can involve any lithology. Internally, the beds are mainly coherent in slides, apart from a shear zone along the base, compressional features in the toe region and tensional structures at the head. There is a more pervasive bed disruption in slumps including several types of folds, thrusts, balls, overfolds, bed rotation and scar surfaces, although no standard sequence of these structures has yet been identified. The direction of slumping, and hence of the slope, is generally taken as perpendicular to the mean of azimuths of the slump fold axes, and is determined from the sense of overturning (Woodcock, 1976).

Debrites (debris flow deposits, olistostromes) are very variable in nature, ranging from mud dominated with only scattered pebbles or boulders to clast dominated with less than 5% muddy matrix. Bed thickness also varies up to several tens of metres, and appears to be positively correlated with maximum clast size. Debrites may be quite structureless or show part or all of the standard sequence illustrated in the model: (I) sheared fissile-lensoid lamination; (II) fault-, slump- and convolute deformation; and (III) matrix-supported clast-rich zone, with or without water-escape features.

These divisions reflect the complex dynamics of debris flows. In part there may be a sliding mechanism involved resulting in basal shear (I). Continued slow forward advance during top-down freezing of the flow results in fault-fold disruption of the layer immediately overlying the shear zone (II). The upper division (III) represents the semi-rigid plug that was being rafted downslope; where this was more fluid and faster moving, then rapid deposition causes upward escape of pore fluids and the development of sub-vertical water-escape pipes. A number of debrites have been described that are clearly coupled, both vertically and/or laterally, with a capping turbidite.

Turbidites

Three different *turbidite models* have been recognized, each with its own standard sequence of structures through a single depositional unit or bed, and each resulting from turbidity current deposition, in some cases with late-stage flow modification. The individual structural features or divisions for the coarse-grained, medium-grained and fine-grained turbidites are best described by reference to Fig. 8.19. Complete sequences are rarely encountered, with partial sequences (top-absent, mid-absent, base-absent) being the rule. Normal grading is common, together with reverse grading particularly at the base of thick coarse-grained beds, and sequential grading through a series of silt laminae in the finer-grained beds.

Bouma (1962) first presented what has now become the classical model for medium-grained sand–mud turbidites. This was soon interpreted as the result of flow deceleration of relatively low-concentration turbidity currents accompanied by rapid deposition (Division A), followed by a progression of bedforms (Divisions B, C, D) representing fallout during high to low flow regime, and finally deposition from the turbidity current tail together with pelagic/hemipelagic settling (Harms & Fahnstock, 1965; Walker, 1965). The absence of a megaripple division between B and C has been discussed by various authors (see summary in Pickering *et al.*, 1989).

High-concentration flows carrying gravel and coarse sand leave deposits quite different from those of classical turbidites, and are the result of a somewhat different set of depositional processes (Pickering *et al.*, 1989). These include: (1) rapid *en masse* deposition due to increased intergranular friction; (2) inverse grading at base due to grain collisions/dispersive pressure; (3) development of traction carpets, driven by shear from the overriding flow, and sequential deposition by 'freezing'; (4) grain-by-grain deposition from suspension with little subsequent traction transport; (5) formation of irregular stratification by alternate deposition of bedload and suspended load; and (6) syn- and/or post-depositional escape of pore-fluids forming dishes, pipes and other escape features.

Several authors have proposed structural sequences of coarse-grained turbidites (e.g. Hiscott & Middleton, 1979; Hein, 1982; Lowe, 1982) and we have summarized Lowe's (1982) scheme in Fig. 8.19.

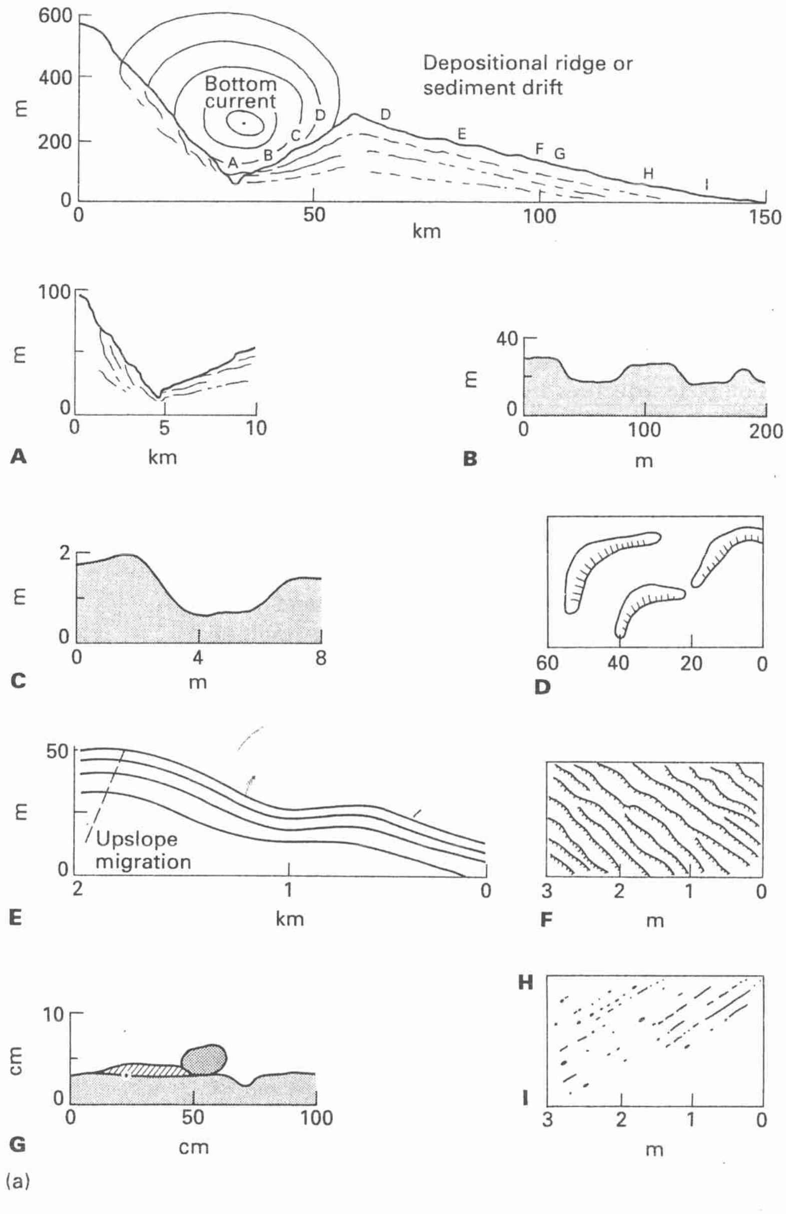

Fig. 8.17 Bottom-current bedforms. (a) Composite diagram. A, moat; B, large furrow; C, small furrow; D, dunes and waves; E, giant sediment waves; F, ripples; G, scour and tail; H, lineation and coarse lag; I, smoothed sediment surface. (Stow, 1981); (b) bottom photograph of valley floor adjacent to Faro Drift, Gulf of Cadiz, showing zones of linguoid ripples, 1, and lineation, 2, (from Faugeres *et al.*, 1985).

There has been some dispute as to whether or not super-critical flow of turbidity currents could produce antidune bedforms at the base (or within) such a sequence (see Hand *et al.*, 1972; Skipper & Bhattacharjee, 1978). However, the beds that were originally described as containing antidunes have subsequently been reinterpreted by Pickering and Hiscott (1985) as flow reversal by reflection and deflection in a constricted basin. Such flow reversal has gained general acceptance from experimental observations (Pantin & Leeder, 1987).

Low-concentration flows, transporting mainly silt- and clay-sized material, may also deposit a regular sequence of structures as a result of waning flow velocity (Piper, 1978; Stow, 1979; Stow & Bowen, 1980; Stow & Shanmugam, 1980). The idealized model (Fig. 8.19) is believed to result from suspension fallout and traction (T_0–T_2), shear-sorting of silt grains and clay flocs in the bottom boundary layer (T_3–T_5), and suspension fallout (T_6–T_8). Many fine-grained turbidites develop only partial sequences (Piper & Stow, 1991), and excessively thick mud

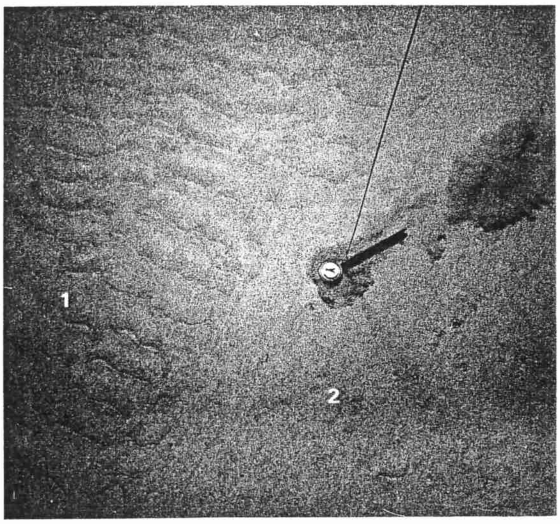

(b)

Fig. 8.17 *Continued*

turbidites appear to show a more complex sequence including multiple repetitions of certain divisions (Porebski *et al.*, 1991).

When a large dilute, mud-charged turbidity current nears the end of its run, perhaps having entered a flat basin plain or having encountered some topographic barrier, two process transitions appear to be possible. The first is for the incoming tail of the turbidity current to provide more and more suspended sediment to the slowing current, so that the concentration builds up and the flow transforms into a high-concentration, slow-moving mud layer (almost a debris flow), that eventually settles out rapidly (or 'freezes') to form a thick structureless mud unit (McCave & Jones, 1988). The second is for flow dilution to continue, and for the finest grained suspension to be thrown up and beyond where the true turbidity current deposits its final thin bed. This material mixes with the basin waters and with the falling pelagic sediment, depositing sufficiently slowly that bioturbation continues but still retaining some of the original characteristics of the parent flow, the 'hemiturbidites' of Stow and Wetzel (1990).

Contourites

The problem of diagnostic lithological features of both modern and ancient *contourites* has long been addressed (Hollister & Heezen, 1972; Stow & Lovell, 1979; Lovell & Stow, 1981; Gonthier *et al.*, 1984; Stow & Faugeres, 1993). It still remains a partly unresolved problem as contourites may mimic sediments deposited by other processes, and bottom-currents may rework, slightly or significantly, other types of deposits.

Depending on the composition of the sediment supply, contourites may be siliciclastic, volcaniclastic or biogenic. Depending on the grain size that the bottom-current is able to transport, contourites range from muddy to sandy, with a range of transitional facies composed of admixtures of sand, silt and clay typically displaying a mottled appearance. Very strong currents may scour the sea floor and result in gravel-lag contourites.

The majority of these deposits are strongly bioturbated, and any primary current structures (lamination, ripples, erosional surfaces) are consequently not well preserved. Better preservation of primary features may occur where there has been an interaction of different processes (e.g. bottom currents and turbidity currents), or more rapid deposition from stronger flows in the case of shallower-water bottom-current deposits.

A standard sequence or contourite model (Fig. 8.20) has been recognized (Faugeres *et al.*, 1984; Gonthier *et al.*, 1984), in which the grain size varies from fine mud, through mottled silty mud to silt and fine sand grade. Where this variation is mirrored by subtle changes in sedimentary structures and concomitant changes in the biogenic/terrigenous composition, then it is possible to interpret the sequence in terms of long-term variation in mean current velocity (Stow *et al.*, 1986). Unlike the standard Bouma (1962) sequence in turbidites, which is the result of instantaneous deposition, the contourite sequence is built up gradually over longer periods, in the order of tens of thousands years.

However, it is not always possible to use grain-size parameters alone as tracers of bottom-current intensity, because various other factors such as variations in terrigenous sediment supply or biogenic productivity may also influence grain size. The interplay of different controlling factors may explain the more irregular 'sequences' or lack of sequences recorded in some drift deposits (Stow & Faugeres, 1993).

8.6 Controls on process and deposit

8.6.1 Introduction

There are many different but overlapping variables that control processes, style and rates of sedimenta-

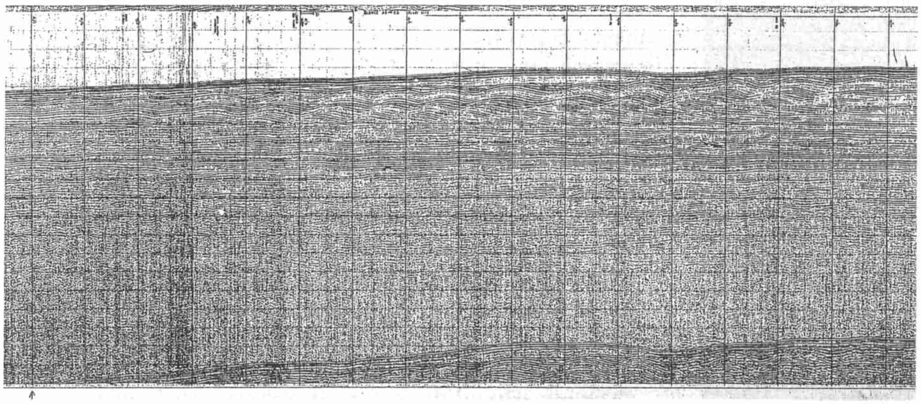

(a)

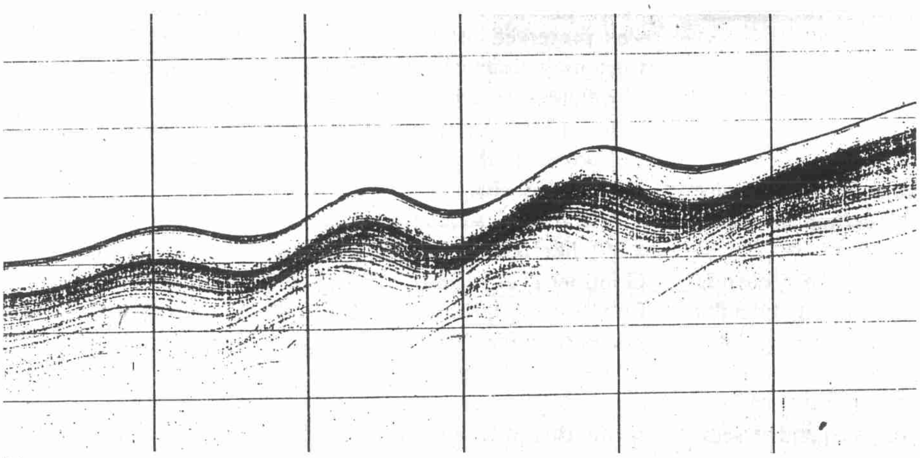

(b)

Fig. 8.18 Sediment waves formed under bottom current and turbidity current flow. (a) Buried sediment wave field, northwest UK Continental Margin (from Richards *et al.*, 1987); (b) detail of sediment waves on backside of small drift in the northeastern area of the Rockall Trough. (From Howe *et al.*, 1993.)

tion in the deep sea. These variables also influence processes in other environments but their effects are necessarily different. In this final section, we briefly review the most important controls including: (1) sediment type and supply; (2) eustatic and local sea-level changes; and (3) tectonic setting and activity. Other factors that have been dealt with in previous sections are: (4) oceanic circulation; (5) sea-water chemistry; and (6) basin size and shape. More wide-ranging controls that we will not discuss specifically here include the relative rates of generation and destruction of oceanic crust, the disposition of the continents and global climate. Good general reviews of controls on deep-sea sedimentation can be found in Stow (1985, 1986), Stow *et al.* (1985), Bouma *et al.* (1985) Jenkyns (1986), and Pickering *et al.* (1989).

8.6.2 Sediment type and supply

Various types of sediment are available for deposition in the deep sea. Terrigenous material is the most abundant worldwide, with muds being between two and ten times as important volumetrically as sands and gravels. Biogenic debris from carbonate reefs and platforms is common at low latitudes, and calcareous and siliceous oozes may drape basins and slopes worldwide and be locally redeposited from areas of

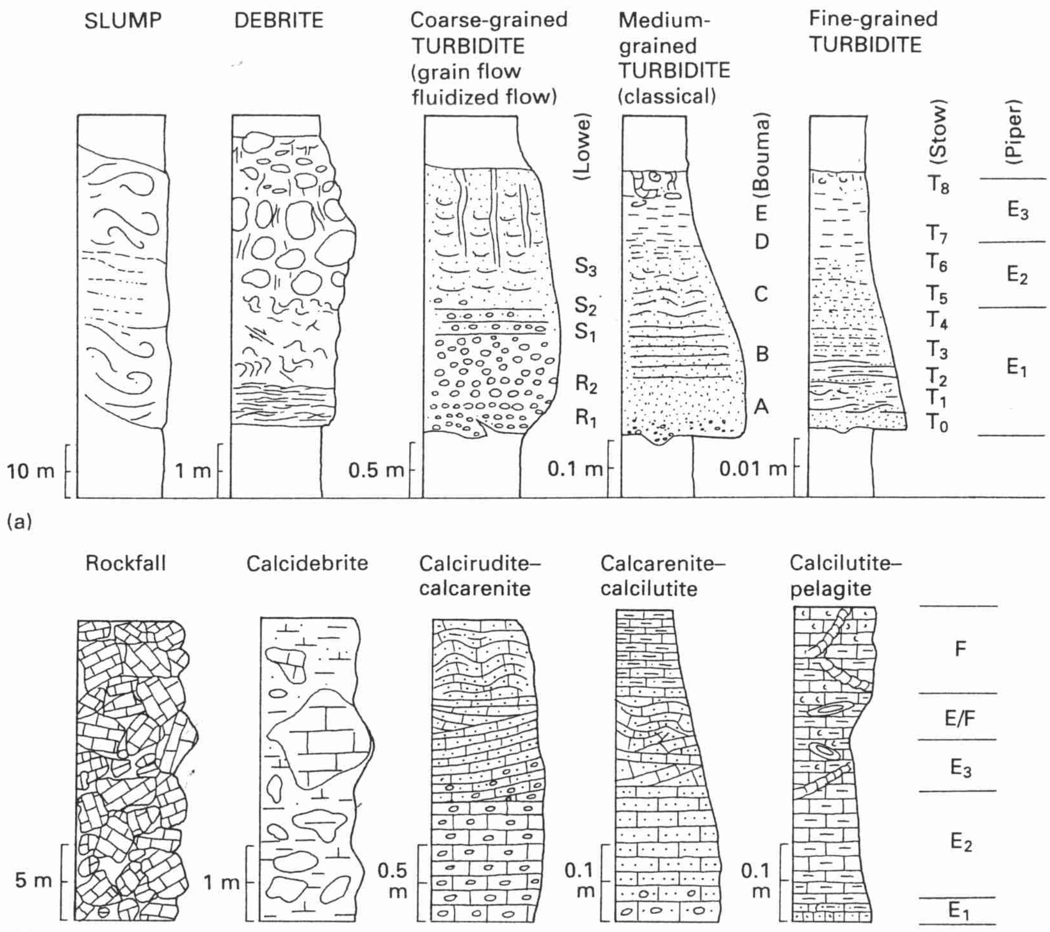

Fig. 8.19 Facies models for resedimented deposits. (a) Resedimented clastic facies models for slumps, debrites and turbidites, showing the idealized structural sequences. The scale bars give an indication only of typical unit thickness, which may vary widely in practice. Grain-size increases to the right for each column. (b) Resedimented carbonate facies models for rock falls, debrites and turbidites. Scale bars give an indication only of typical unit thickness, which may vary widely in practice. Grain size increases to the right for each column. (After Stow, 1986.)

high pelagic accumulation. Evaporites, volcaniclastics and organic-carbon-rich sediments can all occur as turbidites and associated facies. The sediment grain size affects the process and distance of transport and hence the geometry of the deposit. Biogenic particles behave differently from terrigenous grains during transport, so that carbonate facies differ from their clastic counterparts.

The volume and rate at which sediments are supplied to an area, and therefore made available for redeposition, are other important variables. Major river-delta systems, such as the Ganges, Indus, and Mississippi, can provide a large and rapid supply of sediment to the shelf, although the availability of this material for downslope resedimentation will depend on sea level and shelf width. Wave-stirred, canyon-indented shelves will generally provide less sediment to the outer margin. In high latitudes, glaciers and floating ice shelves may greatly increase the supply of terrigenous material to the shelf margin. Low-latitude carbonate platforms and topographic highs covered with pelagic material commonly provide lower rates of sediment supply.

The number and spacing of input points along a

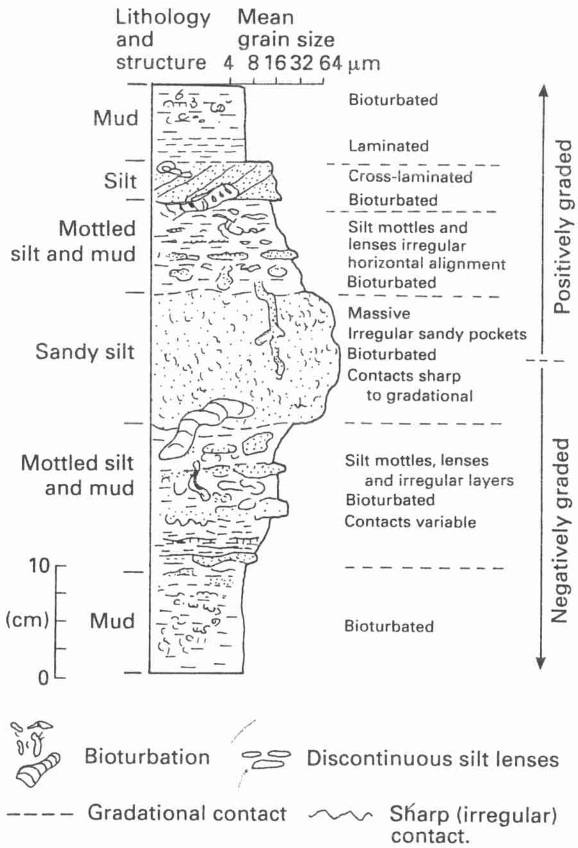

Fig. 8.20 Facies models for bottom current deposits. (After Gonthier *et al.*, 1984.)

given margin will determine whether single or isolated fans are developed, whether an overlapping-fan/slope-apron system is produced, or whether a basin is filled completely or partially.

8.6.3 Eustatic and local sea-level changes

Fluctuation in sea level not only affects the nearshore realm of sedimentation, but also profoundly influences deep-sea depositional and resedimentation patterns. Shoreline sources such as rivers or littoral drift cells either may have direct access to basin slopes during periods of low sea level or indirect access through paralic and continental shelf environments during periods of high sea level.

Sea-level changes may be global (eustatic) or regional in nature. Eustatic fluctuations occur as a result of a change in the total volume of ocean basins or a change in the volume of sea water. Various

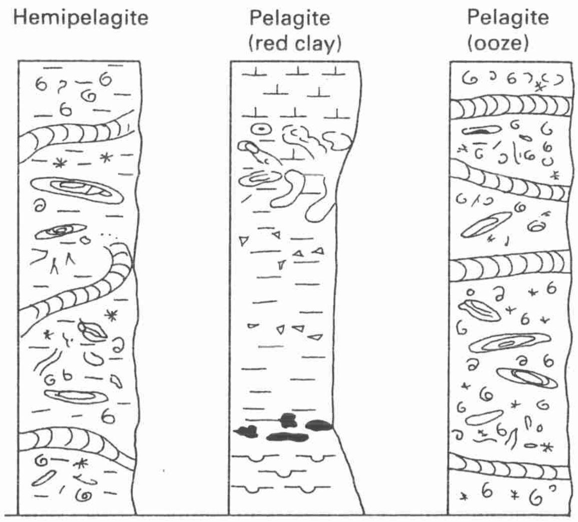

Fig. 8.21 Facies models for pelagites and hemipelagites. (After Stow, 1986.)

attempts have been made to chronicle the eustatic fluctuations and construct an average worldwide curve of sea-level variation (e.g. Haq *et al.*, 1987). Regional fluctuations in sea level that result from local tectonic and isostatic factors can be much greater, and hence locally more significant, than eustatic changes.

Highstands of sea level are associated with an amelioration in climate, increased biological diversity, reduced oxygenation of sea water, shallowing of the CCD, condensed pelagic successions and mud-drape abandonment facies over terrigenous systems. Lowstands, by contrast, are associated with global cooling, widespread unconformities or hiatuses on the shelves and slopes, and increased clastic input into the deep sea.

8.6.4 Tectonic setting and activity

The main tectonic settings in which deep-sea sedimentation occurs include mature passive margins, active rifting margins, convergent margins with or without arc/trench systems, transform margins, marginal seas and back-arc basins, oceanic basins and intracratonic (shelf or mid-continent) basins.

These tectonic settings exert a first-order control on the style and nature of sedimentation by affecting the rates of uplift and denudation, drainage patterns, coastal plain and shelf widths, continental margin gradients, gross sediment budgets, the morphology of receiving basins, and local sea-level changes. The specific tectonic parameters that are particularly important are the size and internal geometry of the basin, including gradients of the base margin and floor. The style and frequency of seismic activity and faulting, both in the original and transitional source areas, are also of primary significance since these factors influence the frequency and volume of sediment gravity flows feeding the basin, for example mature passive margins experience infrequent, but commonly large, earthquakes, which may trigger very large slumps that develop into debris flows and turbidity currents. Frequent earthquakes along active margins do not permit a large build-up of sediment in transitional settings.

8.7 References

Allen J.R.L. 1971. Mixing at turbidity current heads, and its geological implications. *J. Sedim. Petrol.*, **41**, 97–113.

Allen J.R.L. 1982. *Sedimentary Structures: Their Characters and Physical Basis. Developments in Sedimentology*, **30**, I & II, Elsevier, Amsterdam.

Allen J.R.L. 1985. *Principles of Physical Sedimentology.* Allen & Unwin, London.

Asquith J.M. 1979. Nature and origin of the lower continental rise hills, off the east coast of the United States. *Mar. Geol.*, **32**, 165–190.

Athanasiou-Grivas D. 1978. Reliability analysis of earth slopes. *Proc. Soc Engineering Sci. 15th Annual Meeting, Gainesville, University of Florida,*, pp. 453–458.

Bagnold R.A. 1954. Experiments on a gravity-free dispersion of large solid spheres in a Newtonian fluid under shear. *Proc. R. Soc. Lond., A*, **225**, 49–63.

Bagnold R.A. 1962. Auto-suspension of transported sediment; turbidity currents. *Proc. R. Soc. Lond., A,* **265**, 315–319.

Barnes P.M. & Lewis K.B. 1991. Sheet slides and rotational failures on a convergent margin: the Kidnappers Slide, New Zealand. *Sedimentology*, **38**, 205–221.

Biscaye P.E. & Eittreim S.L. 1977. Suspended particulate loads and transports in the nepheloid layer of the abyssal Atlantic Ocean. *Mar. Geol.*, **23**, 155–72.

Bouma A.H. 1962. *Sedimentology of Some Flysch Deposits.* Elsevier, Amsterdam.

Bouma A.H., Barnes N.E. & Normark W.R. (eds). 1985. *Submarine fans and related turbidite systems.* Springer, New York.

Bowen A.J., Normark W.R. & Piper D.J.W. 1984. Modelling of turbidity currents on Navy Submarine Fan, California Continental Borderland. *Sedimentology*, **31**, 169–85.

Carson M.A. & Kirkby M.J. 1972. *Hillslope Form and Process.* Cambridge University Press, Cambridge.

Cheney R.E., Marsh J.G. & Beckley B.D. 1983. Global mesoscale variability from collinear tracks of SEASAT altimeter data. *J. Geophys. Res.* **88**, 4343–4354.

Chough S. & Hesse R. 1976. Submarine meandering talweg and turbidity currents flowing for 4000 km in the Northwest Atlantic Mid-ocean Channel, Labrador Sea. *Geology*, **4**, 529–533.

Curray J.R. & Moore D.G. 1971. Growth of the Bengal deep-sea fan and denudation in the Himalayas. *Bull. Geol. Soc. Am.*, **82**, 563–572.

Curray J.R. & Moore D.G. 1974. Sedimentary and tectonic processes in the Bengal deep-sea fan and geosyncline. In: Burk C.A. & Drake C.L. (eds) *The Geology of Continental Margins* pp. 617–627. Springer, New York.

Damuth J.E. 1975. Echo-character of the western equational Atlantic floor and its relationship to the dispersal and distribution of terrigenous sediments. *Mar. Geol.*, **18**, 17–45.

Dingle R.V. 1977. The anatomy of a large submarine slump on a sheared continental margin (SE Africa). *J. Geol. Soc. Lond.*, **134**, 293–310.

Dott R.H. Jr 1963. Dynamics of subaqueous gravity depositional processes. *Bull. Am. Ass. Petrol. Geol.*, **47**, 104–128.

Dowdeswell J.A. & Scourse J.D. (eds). 1990. *Glacimarine Environments: Processes and Sediments. Geol. Soc. Spec. Publ.*, **53**. Geological Society Publishing House, Bath.

Drake D.E., Hatcher P.G. & Keller G.H. 1978. Suspended particulate matter and mud deposition in Upper Hudson submarine canyon. In: Stanley D.J. & Kelling G. (eds) *Sedimentation in submarine canyons, fans, and trenches,* pp. 33–41. Dowden, Hutchinson & Ross, Stroudsberg, Philadelphia.

Eittreim S. & Ewing M. 1972. Suspended particulate matter in the deep waters of the North American Basin. In: Gordon A.L. (ed.) *Studies in Physical Oceanography*, **2**, 123–168. Gordon & Breach, New York.

Eittreim S., Thorndike E.M. & Sullivan L. 1976. Turbidity distribution in the Atlantic Ocean. *Deep-Sea Res.*, **23**, 1115–1128.

Embley R.W. 1980. The role of mass transport in the distribution and character of deep-ocean sediments with special reference to the North Atlantic. *Mar. Geol.*, **38**, 23–50.

Embley R.W., Hooje P.J., Lonsdale P., Mayer L. & Tucholke B.E. 1980. Furrowed mud-waves on the western Bermuda rise. *Bull Geol. Soc. Am.*, **91**, 731–740.

Faugeres J.C., Gonthier E. & Stow D.A.V. 1984. Contourite drift molded by deep Mediterranean outflow. *Geology*, **12**, (5) 296–300.

Flood R.D. & Shor A.N. 1988. Mud waves in the Argentine basin and their relationship to regional bottom circulation patterns. *Deep-Sea Res.*, **35**, 943–972.

Fukushima Y., Parker G. & Pantin H.M 1985. Prediction of ignitive turbidity currents in Scripps Submarine Canyon. *Mar. Geol.*, **67**, 55–81.

Gardner W.D. & Sullivan L.G. 1981. Benthic storms: temporal variability in a deep ocean nepheloid layer. *Science*, **213**, 329–331.

Gill A.E. 1973. Circulation and bottom water production in the Weddell Sea. *Deep-Sea Res.*, **20**, 111–140.

Goldberg E.D. (ed.) 1974. *The Sea, Vol 5 (Marine Chemistry).* Wiley-Interscience, New York.

Gonthier E.G., Faugeres J.C. & Stow D.A.V. 1984. Contourite facies of the Faro Drift, Gulf of Cadiz. In: Stow D.A.V. and Piper D.J.W. (eds) *Fine-grained Sediments: Deep-water Processes and Facies. Geol. Soc. (Lond.) Spec. Publ.*, **15**, 275–292. Blackwell Scientific Publications, Oxford.

Hampton M.A. 1972. The role of subaqueous debris flow in generating turbidity currents. *J. Sedim. Petrol.*, **42**, 775–793.

Hampton M.A. 1975. Competence of fine-grained debris flows. *J. Sedim. Petrol.*, **45**, 834–844.

Hampton M.A. 1979. Buoyancy in debris flows. *J. Sedim. Petrol.*, **49**, 753–758.

Hand B.M., Middleton G.V. & Skipper K. 1972. Antidune cross-stratification in a turbidite sequence, Cloridorme Formation, Gaspe, Quebec. *Sedimentology*, **18**, 135–138.

Haq B.U., Hardenbol J. & Vail P.R. 1987. Chronology of fluctuating sea levels since the Triassic. *Science*, **235**, 1156–1167.

Harms J.C. & Fahnestock R.K. 1965. Stratification, bed forms and flow phenomena (with an example from the Rio Grande). In: Middleton G.V. (ed.) *Primary Sedimentary Structures and their Hydrodynamic Interpretation.* Spec. Publ. Soc. Econ. Paleont. Mineral, **12**, 84–115. SEPM, Tulsa.

Hay A.E. 1983. On the frontal speeds of internal gravity surges on sloping boundaries. *J. Geophys. Res.*, **88**, 751–754.

Heezen B.C. & Ewing M. 1952. Turbidity currents and submarine slumps, and the 1929 Grand Banks earthquake. *Am. J. Sci.*, **250**, 849–873.

Heezen B.C. & Hollister C.D. 1971. *The Face of the Deep.* Oxford University Press, New York.

Heezen B.C., Ericson D.B. & Ewing M. 1954. Further evidence for a turbidity current following the 1929 Grand Banks earthquake. *Deep-Sea Res.*, **1**, 193–202.

Heezen B.C., Hollister C.D. & Ruddiman W.F. 1966. Shaping of the continental rise by deep geostrophic contour currents. *Science*, **152**, 502–508.

Hein F.J. 1982. Depositional mechanisms of deep-sea coarse clastic sediments, Cap Enrage Formation, Quebec. *Can J. Earth Sci.*, **19**, 267–287.

Hein F.J. & Gorsline D.S. 1981. Geotechnical aspects of fine-grained mass flow deposits: California Continental Borderland. *Geo-Marine Lett.*, **1**, 1–5.

Hill P.R. 1984. Sedimentary facies of the Nova Scotian upper and middle continental slope, offshore eastern Canada. *Sedimentology*, **31**, 293–309.

Hill P.R., Moran K.M. & Blasco S.M. 1982. Creep deformation of slope sediments in the Canadian Beaufort Sea. *Geo-Mar. Lett.*, **2**, 153–70.

Hiscott R.N. & Middleton G.V. 1979. Depositional mechanics of thick-bedded sandstones at the base of a submarine slope, Tourelle Formation (Lower Ordovician), Quebec, Canada. In: Doyle L.J. & Pilkey O.H. (eds) *Geology of Continental Slopes. Spec. Publ. Soc. Econ. Paleont. Mineral*, **27**, 307–326. SEPM, Tulsa.

Hjulstrom F. 1939. Transportation of detritus by moving water. In: Trask P.D. (ed.) *Recent Marine Sediments: A Symposium. Spec. Publ. Soc. Econ. Paleont. Mineral*, **4**, 5–31. SEPM, Tulsa.

Hollister C.D. & Heezen B.C. 1972. Geological effects of bottom currents: western North Atlantic. In: Gordon A.L. (ed.) *Studies in Physical Oceanography*, **2**, pp. 37–66. Gordon and Breach, New York.

Hollister C.D. & McCave I.N. 1984. Sedimentation under deep-sea storms. *Nature*, **309**, 220–225.

Hollister C.D., Flood R.D., Johnson D.A., Lonsdale P. & Southard J.B. 1974. Abyssal furrows and hyperbolic echo-traces on the Bahama Outer Ridge. *Geology*, **2**, 395–400.

Hughes Clarke J.E., Shor A.N., Piper D.J.W. & Mayer L.A. 1990. Large-scale current-induced erosion and deposition in the path of the 1929 Grand Banks turbidity current. *Sedimentology*, **37**, 613–629.

Jenkyns H.C. 1986. Pelagic environments. In: Reading H.G. (ed.) *Sedimentary Environments and Facies*, 2nd edn, pp. 343–397. Blackwell Scientific Publications, Oxford.

Johns D.R. 1978. Mesozoic carbonate rudites, megabreccias and associated deposits from central Greece. *Sedimentology*, **25**, 561–573.

Johnson A.M. 1970. *Physical Processes in Geology.* Freeman, Cooper, San Francisco.

Johnson A.M. 1984. (with contributions by Rodine J.R.) Debris flow. In: Brunsden D. & Prior D.B. (eds) *Slope Instability*, pp. 257–362. Wiley, New York.

Jones M.E. & Preston R.M.F. (eds) 1987. *Deformation of Sediments and Sedimentary Rocks. Geol. Soc. (Lond.) Spec. Publ.*, **29**. Blackwell Scientific Publications, Oxford.

Karlsrud K. & Edgers L. 1982. Some aspects of submarine slope stability. In: Saxov S. & Nieuwenhuis J.K. (eds) *Marine Slides and Other Mass Movements*, pp. 63–81. Plenum Press, New York.

Kenter J.A.M. 1990. Carbonate platform flanks: slope angle and sediment fabric. *Sedimentology*, **37**, 777–794.

Killworth P.D. 1973. A two dimensional model for the formation of Antarctic bottom water. *Deep-Sea Res.*, **20**, 941–971.

Kolla V., Eittreim S., Sullivan L., Kostecki J.A. & Burckle L.H. 1980. Current-controlled abyssal microtopography and sedimentation in Mozambique basin, Southwest

Indian Ocean. *Mar. Geol.*, **34**, 171–206.

Komar P.D. 1969. The channelized flow of turbidity currents with application to Monterey deep-sea fan channel. *J. Geophys. Res.*, **74**, 4544–4558.

Komar P.D. 1971. Hydraulic jumps in turbidity currents. *Bull. Geol. Soc. Am.*, **82**, 1477–1488.

Krause D.C., White W.C., Piper D.J.W. & Heezen B.C. 1970. Turbidity currents and cable breaks in the western New Britain Trench. *Bull. Geol. Soc. Am.*, **81**, 2153–2160.

Kuenen Ph.H. (1967) Emplacement of flysch-type sand beds. *Sedimentology*, **9**, 203–243.

Lafond E.C. 1962. Internal waves. In: Hill M.N. (ed.) *The Sea*, Vol. 1, pp. 731–751. Wiley Interscience, London.

Lee H.J. 1989. Undersea landslides: extent and significance in the Pacific Ocean. In: Brabb E.E. & Harrod B.L. (eds) *Landslides: Extent and Economic Significance*, pp. 367–380. Proc. 28th Int. Geol. Cong., Symposium on Landslides.

Lewis K.B. 1971. Slumping on a continental slope inclined at 1°–4°. *Sedimentology*, **16**, 97–110.

Lonsdale P. & Hollister C.D. 1979. A near-bottom traverse of Rockall Trough: hydrographic and geologic inferences. *Oceanologica Acta*, **31**, 91–105.

Lovell J.P.B. & Stow D.A.V. 1981. Identification of ancient sandy contourites. *Geology*, **9**, 347–349.

Lowe D.R. 1975. Water escape structures in coarse-grained sediments. *Sedimentology*, **22**, 157–204.

Lowe D.R. 1976. Subaqúeous liquified and fluidized sediment flows and their deposits. *Sedimentology*, **23**, 285–308.

Lowe D.R. 1979. Sediment gravity flows: their classification and some problems of application to natural flows and deposits. In: Doyle L.J. & Pilkey O.H. (eds) *Geology of Continental Slopes. Spec. Publ. Soc. Econ. Paleont. Mineral*, **27**, 75–82. SEPM, Tulsa.

Lowe D.R. 1982. Sediment gravity flows: II. Depositional models with special reference to the deposits of high-density turbidity currents. *J. Sedim. Petrol.*, **52**, 279–297.

Luyten J.R. (1977) Scales of motion in the deep Gulf Stream and across the Continental Rise. *J. Mar. Res.*, **35**, 49–74.

Malinverno A., Ryan W.B.E., Auffret G.I. & Pautot G. 1988. Sonar images of the path of recent failure events on the continental margin off Nice, France. *Spec. Pap. Geol. Soc. Am.*, **229**, 59–75.

Mariani M., Argnani A., Roveri M. & Trincardi F. 1993. Sediment drifts and erosional surfaces in the central Mediterranean: seismic evidence of bottom current activity. *Sedim. Geol.*, **82**, 207–220.

Marjanac T. 1985. Composition and origin of the megabed containing huge clasts, flysch formation, middle Dalmatia, Yugoslavia. In: *Abstracts and Poster Abstracts*, pp. 270–273. *6th European Regional Meeting, Lleida, Spain, Int. Assoc. Sedimentologists.*

McCave I.N. 1972. Transport and escape of fine-grained sediment from shelf areas. In: Swift D.J.P., Duane D.B. & Pilkey O.H. (eds) *Shelf Sediment Transport: Process and Pattern*. pp. 225–248. Hutchinson & Ross, Stroudsburg PA.

McCave I.N. 1984. Erosion, transport and deposition of fine-grained marine sediments. In: Stow D.A.V. & Piper D.J.W. (eds) *Fine Grained Sediments: Deep-Water Processes and Facies. Spec. Publ. Geol. Soc. Lond.*, **15**, 35–69. Blackwell Scientific Publications, Oxford.

McCave I.N. & Jones P.N. 1988. Deposition of ungraded muds from high-density non-turbulent turbidity currents. *Nature*, **333**, 250–252.

McCave, I.N. & Swift S.A. 1976. A physical model for the rate of deposition of fine-grained sediments in the deep sea. *Bull. Geol. Soc. Am.*, **87**, 541–546.

McCave I.N. & Tucholke B.E. 1986. Deep current-controlled sedimentation in the western North Atlantic. In: Vogt P.R. & Tucholke B.E. (eds) *The Geology of North America, Vol. M: The Western North Atlantic Region, Decade of North American Geology*, Geology Society of America, pp. 451–468. Boulder, Colorado.

McCave I.N., Londsdale P.F., Hollister C.D. & Gardner W.D. 1980. Sediment transport over the Hatton and Gardar contourite drifts. *J. Sedim. Petrol.*, **50**, 1049–1062.

McLean S.R. 1985. Theoretical modelling of deep-ocean sediment transport. *Mar. Geol.*, **66**, 243–265.

Menard H.W. 1964. *Marine Geology of the Pacific*. McGraw Hill, New York.

Middleton G.V. 1966a. Experiments on density and turbidity currents: I. Motion of the head. *Can. J. Earth Sci.*, **3**, 523–546.

Middleton G.V. 1966b. Experiments on density and turbidity currents: II. Uniform flow of density currents. *Can. J. Earth Sci.*, **3**, 627–637.

Middleton G.V. 1966c. Small scale models of turbidity currents and the criterion for auto-suspension. *J. Sedim. Petrol.*, **36**, 202–208.

Middleton G.V. 1967. Experiments on density and turbidity currents: III. Deposition of sediment. *Can. J. Earth Sci.*, **4**, 475–505.

Middleton G.V. & Hampton M.A. 1973. Sediment gravity flows: mechanics of flow and deposition. In: Middleton G.V. & Bouma A. H. (eds) *Turbidites and Deep Water Sedimentation*, pp. 1–38. *Short Course Notes, Pacific Sect. Soc. Econ. Paleont. Mineral.*

Middleton G.V. & Hampton M.A. 1976. Subaqueous sediment transport and deposition by sediment gravity flows. In: Stanley D.J. & Swift D.J.P. (eds) *Marine Sediment Transport and Environmental Management*, pp. 197–218. John Wiley, New York.

Middleton G.V. & Southard J.B. 1984. *Mechanics of sediment transport*. 2nd edn. Soc. Econ. Paleont. Mineral. Eastern Section Short Course No. 3, Providence.

Middleton G.V. & Southard J.B. 1978. *Mechanics of Sedi-*

ment Movement. SEPM Short Course, **3**. Tulsa.

Miller M.A., McCave I.N. & Komar P.D. 1977. Threshold of sediment motion under unidirectional currents. *Sedimentology*, **24**, 507–528.

Moore D.G. 1961. Submarine slumps. *J. Sedim. Petrol.*, **31**, 343–57.

Moore D.G. 1977. Submarine slides. In: Voight B. (ed.) *Rockslides and Avalanches*, Vol. 1. *Developments in Geotechnical Engineering*, **14A**, 563–604.

Morgenstern N. 1967. Submarine slumping and the initiation of turbidity currents. In: Richards A.F. (ed.) *Marine Geotechnique*, pp. 189–220. University of Illinois Press, Urbana.

Nardin T.R., Hein F.J., Gorsline D.S. & Edwards B.D. 1979. A review of mass movement processes, sediment and acoustic characteristics and contrasts in slope and base-of-slope systems versus canyon–fan–basin floor systems. In: Doyle L.J. & Pilkey O.H. Jr. (eds) *Geology of Continental Slopes. Spec. Publ. Soc. Econ. Paleont. Mineral.*, **27**, 61–73. SEPM, Tulsa.

Nelson C.H. & Kulm L.D. 1973. Submarine fans and channels. In: *Turbidites and Deep Water Sedimentation*, pp. 39–78. *Soc. Econ. Paleont. Mineral, Pacific Section, Short Course*. Anaheim.

Neuman G. 1968. *Ocean Currents*. Elsevier, Amsterdam.

Normark W.R., Hess G.R., Stow D.A.V. & Bowen A.J. 1980. Sediment waves on the Monterey Fan levees: a preliminary physical interpretation. *Mar. Geol.*, **37**, 1–8.

Normark W.R., Piper D.J.W. & Hess G.R. 1979. Distributary channels, sand lobes, and mesotopography of Navy Submarine Fan, California Borderland, with applications to ancient fan sediments. *Sedimentology*, **26**, 749–774.

Nowell A.R.M. & Hollister C.D. (eds) 1985. Deep Ocean sediment transport. *Mar. Geol.*, **66**, 1–4.

Open University. 1984. *Oceanography, Units 11 and 12, Sediments*. The Open University Press, Milton-Keynes.

Pantin H.M. 1979. Interaction between velocity and effective density in turbidity flow: phase plane analysis, with criteria for autosuspension. *Mar. Geol.*, **31**, 59–99.

Pantin H.M. & Leeder M.R. 1987. Reverse flow in turbidity currents: the role of internal solitions. *Sedimentology*, **34**, 1143–1155.

Pickering K.T. & Hiscott R.N. 1985. Contained (reflected) turbidity currents from the Middle Ordovician Cloridorme Formation, Quebec, Canada: an alternative to the antidune hypothesis. *Sedimentology*, **32**, 373–394.

Pickering K.T., Hiscott R.N. & Hein F.J. 1989. *Deep Marine Environments: Clastic Sedimentation and Tectonics*. Unwin Hyman, London, 416 pp.

Pierson T.C. 1981. Dominant particle support mechanisms in debris flows at Mt Thomas, New Zealand, and implications for flow mobility. *Sedimentology*, **28**, 49–60.

Piper D.J.W. 1978. Turbidite muds and silts on deep sea fans and abyssal plains. In: Stanley D.J. & Kelling G. *Sedimentation in Submarine Canyons, Fans and Trenches*, pp. 163–175. Dowden, Hutchinson & Ross, Stroudsburg, PA.

Piper D.J.W. & Normark W.R. 1982. Effects of the 1929 Grand Banks earthquake on the continental slope off eastern Canada. In: *Current Research, Part B. Geol. Surv. Can. Pap.*, **82–1B**.

Piper D.J.W. & Stow D.A.V. 1991. Fine-grained turbidites. In: Einsele G. & Seilacher A. (eds) Cycles and Events in Stratigraphy, pp. 360–376, 2nd edn. Springer-Verlag, Berlin.

Piper D.J.W., Normark W.R. & Stow D.A.V. 1984. The Laurentian Fan–Sohm Abyssal Plain. *Geol. Mar. Lett.*, **3**, 141–146.

Porebski S.J., Meischner D. & Gorlich K. 1991. Quaternary mud turbidites from the South Shetland Trench (West Antarctica): recognition and implications for turbidite facies modelling. *Sedimentology*, **38**, 691–715.

Prior D.B. & Suhayda J.N. 1979a. Submarine landslide morphology and development mechanisms, Mississippi Delta. *Proc. 11th Conf. Ocean Technol., Paper OTC 3482*, 1055–1058.

Prior D.B. & Suhayda J.M. 1979b. Application of infinite slope analysis to subaqueous sediment instability, Mississippi Delta. *Engng. Geol.*, **14**, 1–10.

Rattay M. 1960. On the coastal generations of internal tides. *Tellus*, **12**, 54.

Redbourn L., Bull J., Scrutton R.A. & Stow D.A.V. 1993. Channels, echocharacter mapping and tectonics from 3.5 kltz profiles, distal Bengal Fan. *Mar. Geol.* (in press).

Richardson M.J., Wimbush M. & Mayer L. 1981. Exceptionally strong near-bottom flows on the continental rise off Nova Scotia. *Science*, **213**, 887–888.

Richardson P.L. 1983. Eddy kinetic energy in the North Atlantic from surface drifters. *J. Geophys. Res.*, **88**, 4355–4367.

Saxov S. & Nieuwenhuis J.K. (eds) 1982. *Marine Slides and Other Mass Movements*. Plenum Press, New York.

Schwarz H.-U. 1982. Subaqueous slope failures — experiments and modern occurrences. *Contrib. Sedimentol.*, **11**.

Shepard F.P. 1973. *Submarine Geology*, 3rd edn. Harper and Row, New York.

Shepard F.P. & Dill R.F. 1966. *Submarine Canyons and Other Sea Valleys*. Rand McNally, Chicago.

Shepard F.P., Marshall N.F., McLoughlin P.A. & Sullivan G.G. 1979. Currents in submarine canyons and other seavalleys. *Stud. Geol. Am. Ass. Petrol. Geol.*, **8**.

Shepard F.P., McLoughlin P.A., Marshall N.F. & Sullivan G.G. 1977. Current-meter recordings of low-speed turbidity currents. *Geology*, **5**, 297–301.

Shields A. 1936. Mitt. Preuss. Vers. Anst. Wasserb. u. Schiffb., Berlin, Heft 26.

Shor A., Lonsdale P., Hollister C.D. & Spencer D. 1980. Charlie–Gibbs fracture zone: bottom-water transport and its geologic effects. *Deep-Sea Res.*, **27A**, 325–345.

Shor A.N., Piper D.J.W., Hughes Clarke J.E. & Mayer L.A.

1990. Giant flute-like scour and other erosional features formed by the 1929 Grand Banks turbidity current. *Sedimentology*, **37**, 631–645.

Shultz A.W. 1984. Subaerial debris-flow deposition in the Upper Paleozoic Cutter Formation. *J. Sedim. Petrol.*, **54**, 759–72.

Simm R.W., Weaver P.P.E., Kidd R.B. & Jones E.J.W. 1991. Quaternary mass movement on the lower continental rise and abyssal plain off western Sahara. *Sedimentology*, **38**, 27–40.

Simpson J.E. 1969. A comparison between laboratory and atmospheric density currents. *Q.J.R. Met. Soc.*, **95**, 758–765.

Simpson J.E. 1972. Effects of the lower boundary on the head of a gravity current. *J. Fluid Mech.*, **53**, 759–768.

Simpson J.E. 1982. Gravity currents in the laboratory atmosphere and ocean. *Ann. Rev. Fluid Mech.*, **14**, 213–234.

Skipper K. & Bhattacharjee S.B. 1978. Backset bedding in turbidites: a further example from the Cloridorme Formation (Middle Ordovician), Gaspe, Quebec. *J. Sedim. Petrol.*, **48**, 193–202.

Southard J.B. & Mackintosh M.E. 1981. Experimental test of autosuspension. *Earth Surf. Proc. Landf.*, **6**, 103–111.

Sparks R.S.J., Bonnecaze R.T., Huppert H.E., Lister J.R., Hallworth M.A., Mader H & Phillips J. 1993. Sedimenladen gravity currents with reversing buoyancy. *Earth Planet. Sci. Lett.*, **114**, 243–257.

Stommel H. 1957. A survey of ocean currents theory. *Deep-Sea Res.*, **4**, 149–184.

Stommel H. 1958. The abyssal circulation. *Deep-Sea Res.*, **5**, 80–82.

Stommel H. & Aarons A.B. 1960a. On the abyssal circulation of the World ocean — I. Stationary planetary flow patterns on a sphere. *Deep-Sea Res.*, **6**, 140–154.

Stommel H. & Aarons A.B. 1960b. On the abyssal circulation of the World ocean — II. An idealized model of the circulation pattern and amplitude in oceanic basins. *Deep-Sea Res.*, **6**, 217–233.

Stow D.A.V. 1979. Distinguishing between fine-grained turbidites and contourites on the deep-water margin off Nova Scotia. *Sedimentology*, **26**, 371–387.

Stow D.A.V. 1982. Bottom currents and contourites in the North Atlantic. *Bull. Inst. Geol. Bassin d'Aquitaine*, **31**, 151–166.

Stow D.A.V. 1985. Deep-sea clastics: where are we and where are we going? In: Brenchley P.J. & Williams B.J.P. (eds) *Sedimentology: Recent Developments and Applied Aspects. Geol. Soc. Lond. Spec. Publ.*, **18**, 67–93.

Stow D.A.V. 1986. Deep clastic seas. In: Reading H.G. (ed.) *Sedimentary Environments and Facies*, pp. 398–444, Blackwell Scientific Publications, Oxford.

Stow D.A.V. 1992. *Deep-Water Turbidite Systems.* International Association of Sedimentologists, No. 3. Blackwell Scientific Publications, Oxford.

Stow D.A.V. & Bowen A.J. 1980. A physical model for the transport and sorting of fine-grained sediments by turbidity currents. *Sedimentology*, **27**, 31–46.

Stow D.A.V. & Faugeres J.C. (eds) 1993. Contourites and bottom currents. *Sedim. Geol.*, **82**. Special Issue.

Stow D.A.V. & Lovell J.P.B. 1979. Contourites: their recognition in modern and ancient sediments. *Earth-Sci. Rev.*, **14**, 251–291.

Stow D.A.V. & Shanmugam G. 1980. Sequence of structures in fine-grained turbidites: comparison of recent deep-sea and ancient flysch sediments. *Sedim. Geol.*, **25**, 23–42.

Stow D.A.V. & Wetzel A. 1990. Hemiturbidite: a new type of deep-water sediment. In: Cochran J.R., Stow D.A.V. *et al.* (eds) *Proc. Ocean Drilling Programme Sci. Results*, **116**, 25–34.

Stow D.A.V., Faugeres J.C. & Gonthier E.G. 1986. Facies distribution and drift growth during the late Quaternary, Faro Drift, Gulf of Cadiz. *Mar. Geol.*, **72**, 71–100.

Stow D.A.V., Howell D.G. & Nelson C.H. 1985. Sedimentary, tectonic, and sea-level controls. In: Bouma, A.H., Normark W.R. & Barnes N.E. (eds) *Submarine Fans and Related Turbidite Systems*, pp. 15–22. Springer, New York.

Stow D.A.V., Amano K., Bulson P.S. *et al.* 1990. Sediment facies and processes on the distal Bengal Fan, Leg 116. In: Cochran J.R., Stow D.A.V. *et al.* (eds) *Proc. Ocean Drilling Programme Sci. Results*, **116**, 377–396.

Summerhayes C.P. (ed.) 1992. Upwelling systems: evolution since the early Miocene. *Geol. Soc. (Lond.) Spec. Pub.*, **64**. Geological Society Publishing House, Bath.

Takahashi T. 1981. Debris flow. *Ann. Rev. Fluid Mech.*, **13**, 57–77.

Tolmazin D. 1985. *Elements of Dynamic Oceanography.* Allen and Unwin, London.

Walker R.G. 1965. The origin and significance of the internal sedimentary structures of turbidites. *Proc. Yorks. Geol. Soc.*, **35**, 1–32.

Watkins D.J. & Kraft L.M. 1978. Stability of continental shelf and slope off Louisiana and Texas: geotechnical aspects. In: Bouma A.H., Moore G.T. & Coleman J.M. (eds) *Framework Facies and Oil-Trapping Characteristics of the Upper Continental Margin. Stud. Geol. Am. Ass. Petrol. Geol.*, **7**, 267–286. Tulsa.

Woodcock N.H. 1976. Structural style in slump sheets: Ludlow series, Powys, Wales. J. *Geol. Soc. Lond.*, **132**, 399–415.